Physics 625 - Applied Optics

Second Harmonic Generation Lab

Motivation: The course (lecture and lab) to this point has been almost entirely devoted to linear optics. Reflection, refraction, dispersion, and interference are all linear phenomena. The polarization of a medium or an optical element is linearly proportional to the applied electric field of the light wave over a wide range of field magnitudes. The linearity persists so long as the applied electric field is very much smaller than the electric field which binds the electrons to the nucleus of the atom. The invention of lasers made it possible to generate electric fields in light waves which are not small in comparison to electric fields in atoms. The study of nonlinear optics started a few months after the first laser was built. Nonlinear optics is today one of the most exciting research areas.

Nonlinear optics is so broad that course comparable to Physics 625 would be needed to introduce all of the phenomena which have been discovered. Many of these phenomena have already been applied to basic science or engineering. Lets list a few of the phenomena and applications: frequency doubling, frequency summing, frequency differencing, optical parametric oscillation, Lamb dips, Doppler-free saturation spectroscopy, multiphoton absorption, Doppler-free two photon spectroscopy, stimulated Raman scattering, stimulated Brillouin scattering, quantum beat spectroscopy, coherent anti-Stokes Raman scattering, optical phase conjugation, photon echoes, self induced transparency, optical solitons, squeezed states,...

Theory: This experiment will introduce you to second harmonic generation or frequency doubling. The atomic polarization, P, produced by an electric field E can be expressed using a Taylor series expansion,

$$P = \chi_e E + d(E^2) + \text{higher order terms.}$$

The familiar linear electric susceptibilitiy, χ_e, is directly related to the index of refraction, n, and the dielectric coefficient, ε. The relation in Gaussian units is $n^2 = \varepsilon = 1 + 4\pi\chi_e$. This expansion ignores the vector nature of the polarization and field. The linear electric susceptibility χ_e is represented by a 3x3 tensor in an anisotropic material. The second order nonlinear susceptibility d is represented by a 3x6 tensor in an anisotropic

material. We will briefly ignore the vector nature of the polarization and the field in order to elucidate the phase matching problem.

Part of the induced polarization oscillates and radiates at 2ω, where ω is the angular frequency of the driving wave or the "fundamental frequency".

$$P = \chi_e E + dE^2 \quad \ldots$$
$$= \chi_e E_o \sin\omega t + d (E_o \sin\omega t)^2 + \ldots$$
$$= \chi_e E_o \sin\omega t + d(E_o^2)(1-\cos 2\omega t)/2 + \ldots$$

The key problem to be solved is that wavelets produced in different parts of the medium will not in general combine constructively.

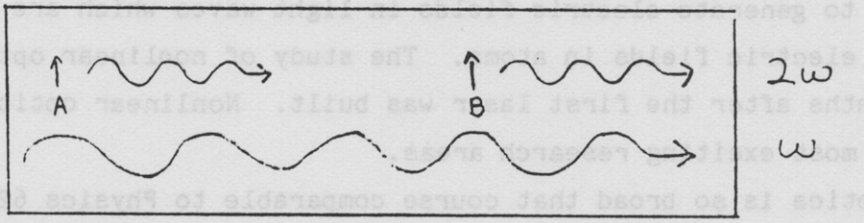

The 2ω polarization and the 2ω wavelets produced at point A are phase locked to the fundamental wave. The same argument can be made at point B. We should not expect that the wavelets from points A and B will combine constructively because of the intrinsic disperison of the material. The index of refraction, and thus phase velocity, are in general different at frequency 2ω and ω. Wavelets from point A will not in general arrive at point B with the desired phase. The solution to the problem is to make use of the anisotropy of the crystal. We use the crystal birefringence to offset its dispersion.

The "phase matching" solution can be understood by taking a detailed look at the linear susceptibility tensor. One choice of axes called the principal axes diagonalizes the linear susceptibility tensor,

$$\begin{vmatrix} \chi_a & 0 & 0 \\ 0 & \chi_b & 0 \\ 0 & 0 & \chi_c \end{vmatrix} .$$

The component of the applied electric field along axis "a" produces a linear polarization $P_a = \chi_a E_a$, and so on. A wave which is polarized such that its electric field is completely along the "a" axis propagates with phase velocity c/n_a where $n_a^2 = 1 + 4\pi\chi_a$ in Gaussian units. The general situation is slightly more complex. Consider a wave propagating such that its wave vector $\bar{k}$ and its

electric field are confined to the a-b plane. Let ϕ be the angle between $\bar{k}$ and the b axis. The index for this wave is

$$\frac{1}{n^2} = \frac{\cos^2\phi}{n_a^2} + \frac{\sin^2\phi}{n_b^2}.$$

Clearly if ϕ is equal to zero the electric field is entirely along the a axis and $n=n_a$. Each possible $\bar{k}$ direction in the crystal can have two waves with different phase velocities. The other solution with $\bar{k}$ vector in the a-b plane has the electric field parallel to the "c" axis and propagates with phase velocity c/n_c.

[This description glosses over many of the fascinating features of solutions to Maxwell's equations in an anisotropic crystal. In many situations $\bar{E}$ is not perfectly orthogonal to $\bar{k}$, and the Poynting vector $\bar{S} = \bar{E} \times \bar{H}$ is not perfectly parallel to $\bar{k}$. The wave fronts slip sideways as they propagate!]

Many, but not all, of the important nonlinear crystals are uniaxial. The ADP or KDP crystal used in this lab is a uniaxial crystal. Two of the principal axes are equivalent in a uniaxial crystal. The third axis is called the optic axis. Both polarizations propagate with the same phase velocity, c/n_o, if $\bar{k}$ is parallel to the optic axis. The index n_o is the ordinary index. If $\bar{k}$ is not parallel to the optic axis, the angle θ between $\bar{k}$ and the optic axis is the polar angle. The indices for a nonzero θ is: n_o for electric field polarization perpendicular to the plane containing $\bar{k}$ and the optic axis, and

$$\frac{1}{n_e^2(\theta)} = \frac{\cos^2\theta}{n_o^2} + \frac{\sin^2\theta}{n_e^2}$$

for electric field polarization in the plane containing $\bar{k}$ and the optic axis. The index n_e is the extraordinary index. It is essential to note that by suitable choice of θ <u>any</u> index between n_o and n_e is accessible.

The solution to the phase matching problem is to chose θ such that

$$n_e(\theta,2\omega) = n_o(\omega).$$

for a negative ($n_e < n_o$) uniaxial crystal such as ADP or KDP. The frequency is an explicit argument to remind us that the indices are frequency dependent and are to be evaluated at different frequencies. This equation is a mathematical statement of the phrase "use birefringence to offset dispersion". The

fundamental wave is chosen to be an ordinary "o" wave and the second harmonic is chosen to be the extraordinary "e" wave in negative uniaxial crystals.

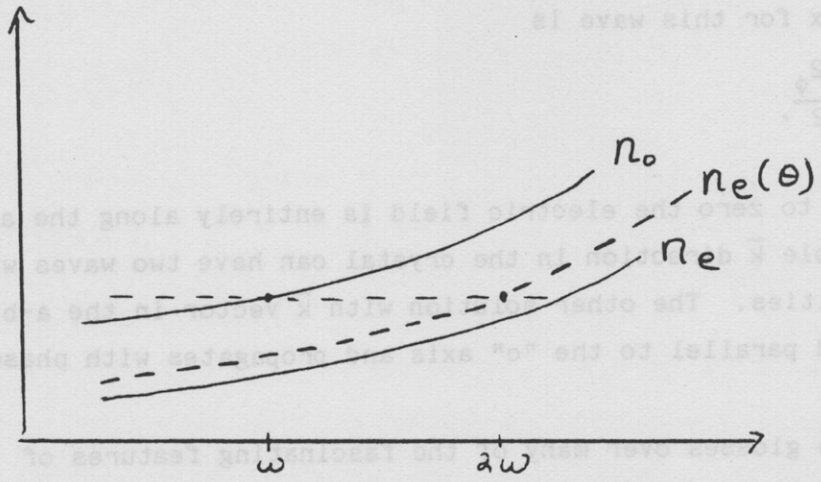

The second harmonic has a polarization orthogonal to the fundamental. The second order nonlinear susceptibility tensor has the necessary anisotropy to couple the orthogonally polarized fundamental and second harmonic waves. The nonlinear polarization in the medium has a component orthogonal to the polarization of "driving" fundamental wave!

Experiment:

(1) Observe frequency doubling in the wave. Use either the dye laser or the Ar^+ ion laser tuned to 528.7 nm. Use a Corning 7-54 filter to block the fundamental wave.

(2) Measure the polar phase matched angle at one or more known fundamental wavelengths. Remember to correct for refraction at the crystal surface. Compare to an angle calculated using the accurate index tables of F. Zernike, J.O.S.A. 54, 1215 (1964).

(3) Verify that the second harmonic power scales as the fundamental power squared.

(4) Experiment with different focal conditions.

Nonlinear Optics

by David Anafi and Joseph P. Machewirth

An overview of harmonic generation and optical mixing in KDP and its isomorphs.

Even though frequency doubling, or second harmonic generation (SHG), was the first significant nonlinear optical phenomenon[1] and still the most important method for producing higher frequency coherent radiation, it is possible to develop a general model in which two electromagnetic waves interact within a dielectric medium. Then, frequency doubling may be considered as a special case where two incident waves are identical waveforms.

To better understand the physics of nonlinear optical effects; it is necessary to investigate the effect of an electric field on the dielectric medium. In the following discussion, we will limit the dielectric media to uniaxial, tetragonal crystals, such as KDP and ADP. We will also limit the crystal media with regard to orientation of the optic (Z) axis. The cartesian coordinate system defined in Figure 1 shows the Z crystallographic axis constrained with the $\bar{i}\bar{k}$ plane.

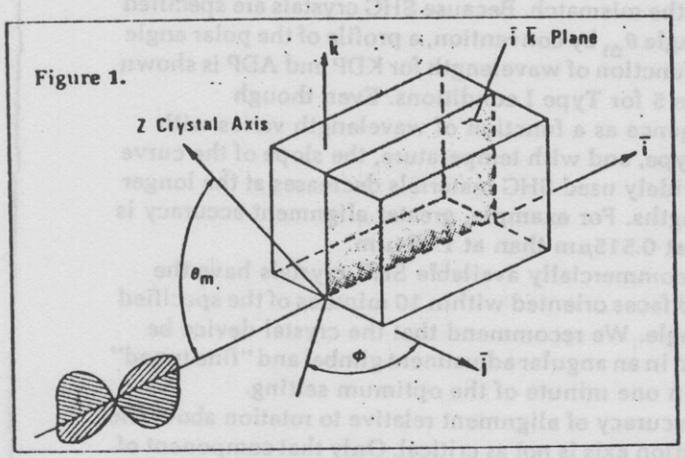

Outlining this effect

Consider the incident waves as electric fields, $\bar{E}_1$ and $\bar{E}_2$, which propagate within the crystal, and express these fields as the summation of components along the crystallographic axis (x,y,z). The presence of these electric fields causes an electric polarization $\bar{P}$ where

$$\bar{P} = e_o \chi \bar{E}_1 \bar{E}_2 \qquad (1)$$

where χ is the susceptibility of the material. For anisotropic crystals like ADP and KDP, χ is an 18 term tensor, but has only three nonvanishing terms (d_{14}, d_{25}, d_{36}).

The linear polarization of the incident and exiting beams must not be confused with the electric polarization $\bar{P}$ that exists only within the crystal media. The induced polarization $\bar{P}$ generates a forced electric field, as well as those of the incident beam (often referred to as free fields). It is the aggregate of the three electric fields that interact with the media, causing the electrons of the molecules to vibrate only in directions along the crystallographic axes. An oscillating electron structure is a radiator, and a third electromagnetic wave is generated, as shown in Figure 2.

There can also be two possible conditions for the linear polarization vectors of the incident beams. If both polarization vectors are parallel and lie in the $\bar{i}\bar{j}$ plane, we can define a condition referred to as Type I. Under Type II conditions, one wave is polarized in the $\bar{i}\bar{j}$ plane and the other lies in the orthogonal $\bar{i}\bar{k}$ plane. Under the former, only the electric polarization along the Z crystal axis contributes to generating a third wave, such that

$$P_z = 2d_{36} E_x E_y \qquad (2)$$

where d_{36} is the susceptibility tensor component. Note that this relationship is limited to crystals of the $\bar{4}\bar{2}m$ point group. A similar relationship can be generated from equation 1 for other classes of nonlinear materials.

Accordingly for Type II conditions the contributing electric polarization components are

$$P_x = 2d_{14} E_y E_z \qquad (3a)$$

$$P_y = 2d_{14} E_x E_z \qquad (3b)$$

To increase the magnitude of the generated wave, the electric polarization must be increased. But constructive interference can only be achieved when dipole radiators

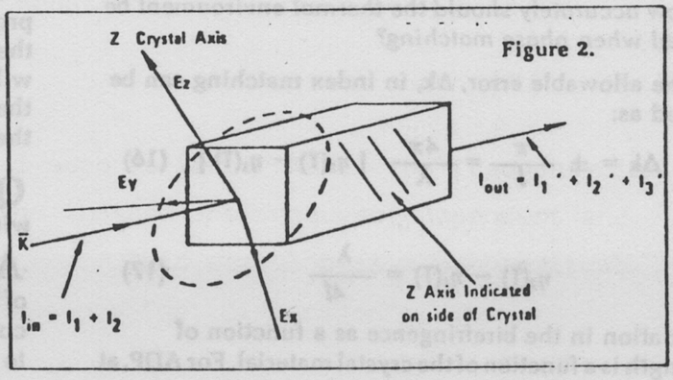

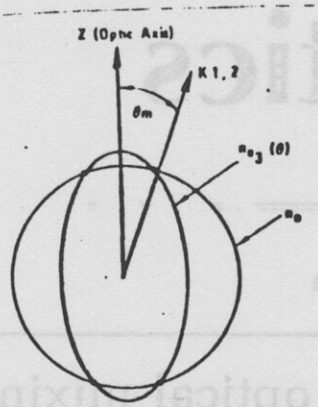

Figure 3.

oscillate in phase. This phase match condition is derived from the equation of momentum conservation:

$$\bar{K}_3 = \bar{K}_1 + \bar{K}_2 \qquad (4)$$

where in general terms:

$$\bar{K}_\omega = \frac{\omega \eta_\omega(\theta)}{C} \qquad (5)$$

ω = the angular frequency of the wave and

$\eta_\omega\theta$ = the refractive index for the wave of frequency as a function of θ.

When equation 4 is solved for Type I conditions, the generated wave will propagate as an e-ray with the two incident waves propagating as o-rays. As a result, equation

The Nonlinear Query

Q *What are the basic parameters that must first be considered when selecting a crystal material?*

A The first and most obvious consideration is the optical transmittance of the material at the wavelengths λ_1, λ_2 and λ_3. A significant bulk absorption will not only reduce the transmittance efficiency of the crystal, but will raise its temperature, an undesirable effect since the refractive indices are temperature dependent. Also, an incident laser with high power density will damage an absorbing crysal media.

Second, to obtain a sufficient conversion efficiency, it is necessary to select a medium with a high nonlinear coefficient.

Finally, the environment in which the device is to be used must be considered. Most nonlinear crystals that can be grown to adequate size are hygroscopic and must be mounted in hermetically sealed cells. These cells are either filled with dry nitrogen or with an index matching fluid.

Q *How do we select the best method of phase matching (temperature versus angle) for a particular application?*

A From the relationships for the intensity of the generated wave I_3, developed in equations 13 through 15, I_3 becomes a function of $\mathrm{Sin}^2\,\theta_m$. Therefore, maximum efficiency is obtained when the incident propagation vector is incident at the angle of 90° to the Z crystal axis. This is the orientation for temperature tuning (see Figure 4). There exists no beam walk-off to disturb the ability to phase match; but there may be other conditions that negate this advantage. For example, the temperature needed to achieve phase matching may exceed the Curie point of the material.

Q *How accurately should the thermal environment be controlled when phase matching?*

A The allowable error, Δk, in index matching can be expressed as:

$$\Delta k = \pm \frac{\pi}{l} = \frac{4\pi}{\lambda}\,[\,\eta_2(T) - \eta_1(T)\,] \qquad (16)$$

where

$$\eta_2(T) - \eta_1(T) = \frac{\lambda}{4l} \qquad (17)$$

The variation in the birefringence as a function of wavelength is a function of the crystal material. For ADP, at room temperature, the literature[4] shows that

$$\frac{d}{dt}(\eta_o - \eta_e) = -4.8 \times 10^{-5}$$

If the crystal length is 10mm and the incident fundamental wavelength is 1.064μm,

$$\frac{\lambda}{4l} = 2.7 \times 10^{-5}$$

Therefore, the allowable ΔT is approximately 1/2°C. It should be noted that when angle phase matching, fluctuations in ambient temperature may be corrected by corresponding variations in the angle θ_m. As the length of the crystal is increased, thermal stability becomes more critical.

Q *When angle phase matching, how accurately must the crystal be aligned?*

A The allowable error in phase matching developed above is a general condition and not dependent on the cause of the mismatch. Because SHG crystals are specified by the angle θ_m by convention, a profile of the polar angle θ_m as a function of wavelength for KDP and ADP is shown in Figure 5 for Type I conditions. Even though birefringence as a function of wavelength varies with crystal type, and with temperature, the slope of the curve for all widely used SHG materials decreases at the longer wavelengths. For example, greater alignment accuracy is needed at 0.515μm than at 1.064μm.

Most commercially available SHG crystals have the polished faces oriented within 10 minutes of the specified polar angle. We recommend that the crystal device be mounted in an angular adjustment gimbal and "fine tuned" to within one minute of the optimum setting.

The accuracy of alignment relative to rotation about the propagation axis is not as critical. Only that component of the incident polarization vector that is properly aligned will contribute to the interaction. For Type I interactions, the incident polarization vector must be aligned at 90° to the $\overline{ik}$ plane.

Q *What range of wavelengths can be frequency doubled with one crystal?*

A Only vignetting of the incident beam limits the range of the polar angle θ that can be obtained with a single angle cut crystal. Still, the angular range is customarily restricted to within 8° because increasing the cross section of a crystal

may be written

$$\eta_{e_3}(\theta_m) = \frac{1}{\omega_3}(\omega_1 \eta_{o_1} + \omega_2 \eta_{o_2}) \qquad (6)$$

Equation 6 provides an expression for the refractive index of the e-ray as it propagates at an angle θ_m, with respect to the crystal optic axis. When K_1 and K_2 are incident at the optimum phase match angle θ_m, all dipole oscillations are in phase. Substituting the value of $\eta_{e3}(\theta)$ from equation 6 into the equation for the unaxial index ellipsiod provides the relationship for θ_m:

$$\frac{1}{\eta_c^2(\theta)} = \frac{\cos^2\theta}{\eta_o^2} + \frac{\sin^2\theta}{\eta_e^2} \qquad (7)$$

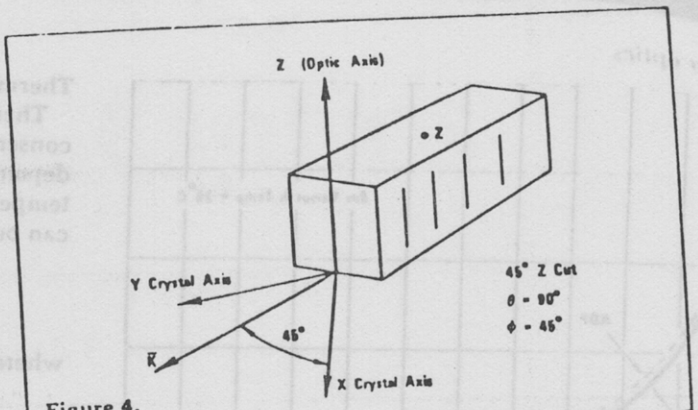

Figure 4.

solely to prevent vignetting increases the cost substantially; Fresnel reflection losses are increased; and most angular adjustment devices are limited to within a 10° range.

To frequency double the lines of a dye laser, we suggest that five crystals be used with different θ_m angles to cover the entire wavelength range. For certain materials, temperature phase matching permits the frequency doubling an extended wavelength range with a single crystal, an advantage usually accompanied by the problems of instrumentation and control.

Q *Why is a Type I angle matched crystal cut with angle ϕ equal to 45°?*

A The maximum interaction is achieved when $E_x = E_y = \sqrt{2/2}\,E$. Figure 6a demonstrates the orientation of a Type I angle cut crystal with respect to the incident beam.

Q *Can second harmonic generation be achieved using the Type II process?*

A The Type II process has proven more efficient than Type I in SHG applications for certain fundamental wavelengths—most significantly, 1.064μm. Since the Type II conversion efficiency is proportional to $\mathrm{Sin}^2\,2\theta_m$, this process is preferred when

$$\mathrm{Sin}^2\,2\theta_m(\mathrm{II}) = 1.8\ \mathrm{Sin}^2\,\theta_m(\mathrm{I})$$

Using the 1.064μm fundamental as an example, $2\theta_m$ (II) equals 118°20' compared with 41°12' for θ_m (I) and

$$\mathrm{Sin}^2\,2\theta_m(\mathrm{II}) > \mathrm{Sin}^2\theta_m(\mathrm{I})$$

A second consideration in favor of the Type II process is the reduction of the mismatch, Δk, due to angular divergence from the phase matched direction by a factor of 2. Here alignment and thermal control become less critical.

In special applications where two different lasers with orthogonally polarized beams are used[6], mixing must be achieved with the Type II process. And, conversion efficiency can be increased with Type II if the output from a single laser is unpolarized. A single linearly polarized fundamental may be equally divided into o- and e-rays by orienting the polarization vector at ±45° with respect to the X axis shown in Figure 6b. Under this condition, the polarization of the harmonic is rotated 45° from the fundamental.

Whenever the required clear aperture of a SHG crystal approaches the limit of growth capability, a Type II angle cut crystal offers an additional advantage of greater yield from the boule since $\phi = 0$. This result is particularly important in laser fusion applications where apertures in excess of 100 mm diameter are desirable.

Q *The most common use of nonlinear devices to date is second harmonic generation. What other applications are possible?*

A Two incident beams of different wavelengths can interact to generate a beam of a third wavelength—a process often referred to as optical mixing or heterodyning. For example, the interaction of 1.06μm and 0.26μm will generate a third harmonic of 1.21 μm[7]. When I_1 and I_2 are added to produce I_3, the incident beams will surrender an equal number of photons in the interaction to generate I_3. When I_1 and I_2 are subtracted, the higher energy photons will generate I_3 and also a stronger I_2.[8]

Q *Should a SHG crystal be utilized intra- or extra-cavity?*

A Most applications for SHG crystals are external to the cavity. The advantage of intra-cavity use (higher output power density) is generally offset by the following factors: 1. In low gain cavities, the insertion loss of the crystal device may be prohibitive; 2. In many cases, the laser cavity will not accept an additional element without costly modification; 3. External focusing lenses may be used to control the incident power density to the crystal without modifying the laser cavity.

Q *What methods are most commonly used to separate the second harmonic from the fundamental beam?*

A In Type I phase matching applications, the fundamental wavelength exits the crystal as an o-ray and the generated wave as an e-ray. This orthogonality relationship can be used to discriminate between the two beams. Calcite, glan-laser or vacuum deposited thin film polarizers can be used to reject the unwanted component. Polarizing beamsplitters can also be used to introduce a divergence between the two components.

Discrimination with polarizers is not always applicable for Type II phase matching. In the Type II interaction, we must take advantage of the dispersive power of prisms or the wavelength selectivity of narrow bandpass optical filters. □

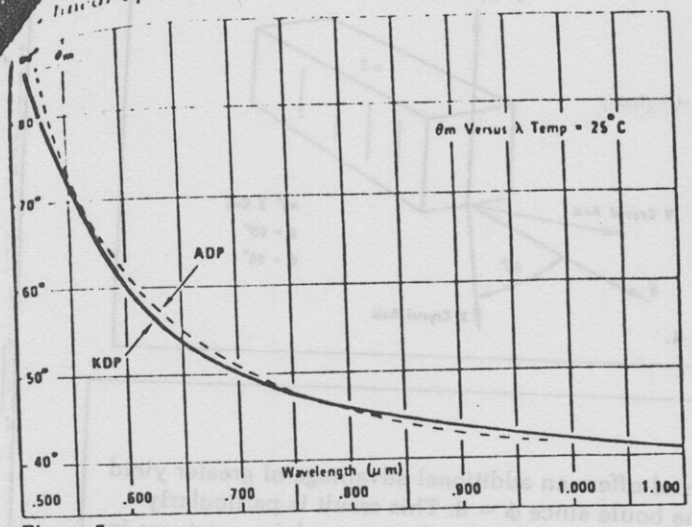

Figure 5.

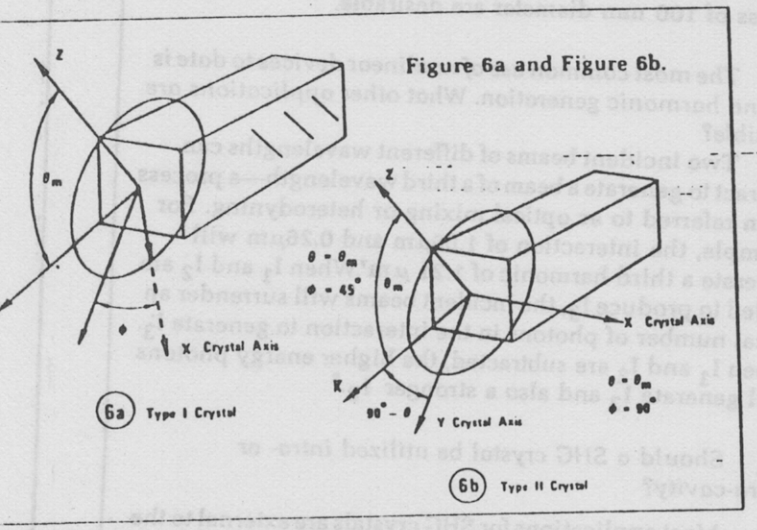

Figure 6a and Figure 6b.

For Type I conditions

$$\sin^2\theta_m = \frac{1/N^2 - 1/\eta_{o_3}^2}{1/\eta_{e_3}^2 - 1/\eta_{o_3}^2} \qquad (8)$$

where we have defined

$$N = \frac{1}{\omega_3}(\omega_1 \eta_{o_1} - \omega_2 \eta_{o_2}) \qquad (9)$$

For the special case of Type I second harmonic generation, where $\omega_1 = \omega_2 = \frac{\omega_3}{2}$ and $\eta_{o1} = \eta_{o2}$:

$$\sin^2\theta_m = \frac{1/\eta_{o_1}^2 - 1/\eta_{o_3}^2}{1/\eta_{e_3}^2 - 1/\eta_{o_3}^2} \qquad (10)$$

If we plot the index surfaces in two dimensions, as shown in Figure 3, there are two solutions for θ_m. As a result, it is evident that the crystal can be oriented two ways, relative to the incident beam, and still satisfy the optimum phase matching requirements. This means that each polished aperture face can be either the entrance or exit face.

Under Type II conditions, where the incident waves are orthogonally plane polarized, the generated wave will propagate as an e-ray with the incident rays as an e- and o-ray. Solving equation 4 for these conditions:

$$\omega_3 \eta_{e_3}(\theta) = \omega_1 \eta_{o_1} + \omega_2 \eta_{e_2}(\theta) \qquad (11)$$

Two solutions for θ_m are obtained when equation 11 is substituted into equation 7. Solutions for specific wavelengths for Type II conditions are presented in the literature.[2,3]

Thermally induced index matching

There is another way to satisfy the conditions for conservation of momentum. In equation 6, we stated a dependence of η_{e3} on the angle θ_m. There also is a temperature dependence for η_{e3} and N. This dependence can be expressed by

$$\eta_{e_3}(T) = \eta_{e_3} + \Delta\eta_{e_3} \qquad (12a)$$

where

$$\Delta\eta_{e_3} = C(\eta_{e_3}^2 + a\eta_{e_3} + b)(298° - T) \qquad (12b)$$

and

η_{e_3} = extraordinary refractive index at 298°K

The constants a, b and c are material dependent and values are presented by Phillips.[4]

Generated wave output: type I process

A general expression that relates the generated wave intensity, I_3, with the input intensities, I_1 and I_2, is given by

$$I_3 = I_1 I_2 \left(\frac{2^9\pi^5 l^2}{C\lambda_3^2 \eta_{o_1}\eta_{o_2}\eta_{o_3}}\right) d_{36}^2 \sin^2\theta_m \qquad (13)$$

where

l = length (cm) of crystal

λ_3 = wavelength (cm of the generated wave)

Note, however, that equation 13 is an approximate relationship that is valid only when I_1 and $I_2 < 1$ megawatt/cm². Under this condition, the conversion efficiency is small enough to assume that the electric fields of I_1 and I_2 are constant across the length of the crystal.

For second harmonic generation where $\lambda_1 = \lambda_2$ and $\eta_{o1} = \eta_{o2} = \eta_{o3}$

$$I_3 = I_1^2 \left(\frac{2^9\pi^5 l^2}{c\lambda_3^2\eta_o^3}\right) d_{36}^2 \sin^2\theta_m \qquad (14)$$

An expression for I_3 SHG that is valid for all input power densities is given by

$$I_3 = I_1 \tanh^2 \sqrt{I_1 d_{36}^2 \left(\frac{2^9\pi^5 l^2}{C\lambda_3^2\eta_o^3}\right)} \sin^2\theta_m \qquad (15)$$

This is an approximate solution where we assume that the bulk absorption of the crystal is negligible and that $l < l_c$ where l_c is the coherent length. Development of similar relationships is provided by N. Bloembergen.[5] □

References

1. Franken, P.A., A.E. Hill, C.W. Peters and G. Weinreich (1961). PHYS. REV. LETTERS. 7:118.
2. Weber, H.P., et al. (1966). J. APPL. PHYS. 37:3584.
3. Okada, M. and S. Ieriri (1971). JAPAN J. APPL. PHYS. 10:808.
4. Phillips, R.A. (1966). J. OPT. SOC. AM. 56:629.
5. Bloembergen, N. (1965). Nonlinear Optics. W.A. Benjamin.
6. Weber, H.P. (1967). J. APPL. PHYS. 38:2231.
7. Massey, G.A. (1974). APPL. PHYS. LETTERS. 24:371.
8. Dewey, C.F. and L.O. Hocker (1971). APPL. PHYS. LETTERS. 18:58.
9. Bates, H.E., (1973). J. OPT. SOC. AM. 63:146.

Meet the authors

Mr. Machewirth is Vice President and Technical Director of Lasermetrics, Inc. in Teaneck, N.J. He received his M.S. in physics from Stevens Institute of Technology. Mr. Anafi is the Senior Scientist at Lasermetrics and received his M.S. in electro-physics from New York University.

Refractive Indices of Ammonium Dihydrogen Phosphate and Potassium Dihydrogen Phosphate between 2000 Å and 1.5 μ

FRITS ZERNIKE, JR.

The Perkin-Elmer Corporation, Optical Maser Department, Norwalk, Connecticut 06852

(Received 21 April 1964)

The refractive indices of ADP and KDP have been measured at 25 wavelengths between 2138 Å and 1.529 μ, and at 24.8°C. The measured values have been corrected to give absolute indices. Curves have been fitted to the measured and to the corrected data.

The measured and the computed data are given both in air and in vacuum. The accuracy of the data is believed to be ±0.00003 or better.

INTRODUCTION

RECENTLY, the discovery of nonlinear optical effects[1] has renewed the interest in the properties of potassium dihydrogen phosphate (KDP) and ammonium dihydrogen phosphate (ADP).

As has been shown by Giordmaine[2] and by Maker *et al.*,[3] the phase velocities of the various waves involved in optical mixing experiments can be matched in a birefringent crystal by proper choice of the angle between the wave vectors and the crystal axis. A precise knowledge of the crystal's refractive indices as a function of wavelength is necessary for that choice. We have measured the refractive indices of both ADP and KDP in air between 2138 Å and 1.529 μ. We have fitted curves to these data both for the absolute indices and for the indices relative to air.

To our knowledge, no measurements as extensive as these have been published. However, in various publications, indices for some wavelengths are given.

The *International Critical Tables*[4] give values for ADP and for KDP for 4860, 5890, and 6560 Å.

Vergnoux[5] has measured the birefringence of ADP and KDP.

TABLE I. Index of refraction of fused silica in air.

Wavelength (Å)	Measured index Zernike	Computed index Rodney and Spindler	Residual×10⁵ Zernike[a]	Residual×10⁵ Rodney and Spindler
3650.15	1.47475	1.47465	+10	+21
4046.56	1.46980	1.46971	+9	+21
4358.35	1.46688	1.46677	+11	+21
5460.74	1.46026	1.46014	+12	+22
5780.12	1.45900	1.45887	+13	
10 139.8	1.45044	1.45030	+14	+23
11 286.6	1.44906	1.44893	+13	
13 672.8	1.44650	1.44622	+28	
13 950.6	1.44607	1.44590	+17	
15 295.2	1.44450	1.44434	+16	+24

[a] Residuals based on results given in column 3.

Vishnevskii and Romanyuk[6] suggest the use of ADP for ultraviolet optical components and give a dispersion equation with four constants.

Dennis and Kingston[7] have measured the indices of KDP at 18 wavelengths between 2536 Å and 1.53 μ with an estimate of error of ±0.002 in the ultraviolet and ±0.004 in the infrared.

EXPERIMENTAL

The refractive indices were measured by the method of known incidence used by Rydberg[8] and more recently by Tilton *et al.*[9]

Prisms of the materials to be measured were inserted in a Perkin-Elmer model 98 monochromator employing a Littrow-type mount. The deviation through each prism was measured for different wavelengths by measuring the angle over which the Littrow mirror had to be rotated to pass a particular wavelength to the exit slit. The screw which rotated the mirror was calibrated by substituting a mirror with two faces at small angles to one another for the Littrow mirror and autocollimating first on one face and then on the other. The autocollimator was a Hilger and Watts 18-in. model with a resolution of ½″. Two mirrors were used, one with an angle of 5° 3′ 14.8″ and the other one with an angle of 30′ 29.4″ between the two faces. These angles were measured on a Watts goniometer.

The angles of the prisms were also measured on this goniometer. Using the calibration of the screw, we measured all the other angles involved. These are: the angle between the exit and the entrance slit, the angle between the incident beam and the Littrow mirror, and the angle of incidence on the prism.

For measurement of the angle between the slits, the Littrow mirror was set perpendicular to the incoming beam with the wavelength drum in one extreme position (0000.0). The drum was then rotated until the beam fell on the exit slit. From this rotation the angle

[1] For a review article see P. A. Franken and J. F. Ward, Rev. Mod. Phys. 35, 23 (1963).
[2] J. A. Giordmaine, Phys. Rev. Letters 8, 19 (1962).
[3] P. D. Maker, R. W. Terhune, M. Nisenoff, and C. M. Savage, Phys. Rev. Letters 8, 21 (1962).
[4] *International Critical Tables* (McGraw-Hill Book Company, Inc., New York, 1926) 1st ed., Vol. VII.
[5] A. Vergnoux, Cahiers Phys. 73, 46 (1956).
[6] V. N. Vishnevskii and N. A. Romanyuk, Opt. i Spectroskopiya 8, 389 (1960) [English transl.: Opt. Spectry (USSR) 8, 389 (1960)].
[7] J. H. Dennis and R. H. Kingston, Appl. Opt. 2, 1334 (1963).
[8] F. Rydberg, Poggendorfs Ann. 14, 45 (1828).
[9] L. W. Tilton, E. K. Plyler, and R. E. Stephens, J. Res. Natl. Bur. Std. (U.S.) 43, 81 (1949).

TABLE II(a). Indices of KDP in air, ordinary ray.

Wavelength[a] (Å)	Source	Observed index	Computed index	Residual $\times 10^4$
2138.560	Zn	1.60177	1.60171	0.6
2288.018	Cd	1.58546	1.58544	0.3
2446.905	Hg	1.57228	1.57236	−0.9
2464.068	Hg	1.57105	1.57114	−1.0
2536.519	Low pressure Hg	1.56631	1.56636	−0.5
2800.869	Zn	1.55263	1.55266	−0.3
2980.628	Cd	1.54618	1.54574	4.4
3021.499	Hg	1.54433	1.54437	−0.4
3125.663	Zn	1.54117	1.54115	0.2
3131.545	Hg	1.54098	1.54098	0.0
3650.146	Hg	1.52932	1.52932	0.1
3654.833	Hg	1.52923	1.52924	−0.1
3662.878	Hg	1.52909	1.52910	−0.1
4046.561	Hg	1.52341	1.52344	−0.2
4077.811	Hg	1.52301	1.52304	−0.4
4358.350	Hg	1.51990	1.51990	−0.0
5460.740	Hg	1.51152	1.51160	−0.8
5769.580	Hg	1.50987	1.50996	−0.9
5790.654	Hg	1.50977	1.50986	−0.9
6328.160	Laser	1.50737	1.50741	−0.4
10 139.75	Hg	1.49535	1.49523	1.2
11 287.04	Hg	1.49205	1.49189	1.6
11 522.76	Laser	1.49135	1.49119	1.7
13 570.70	Hg	1.48455	1.48480	−2.5

[a] The polarizers do not give 100% polarization: therefore, it was sometimes difficult to distinguish a weak line in one direction of polarization from a coinciding strong line in the other direction of polarization. Also, sometimes some of the weaker lines were not observed. This is the reason why some wavelengths are not listed in all of the tables.

between the entrance and the exit slit was determined, using the calibration of the screw.

To measure the angle between the incident beam and the Littrow mirror, the mirror was again set perpendicular to the incoming beam with the drum in one extreme position. (This adjustment was checked by focusing an autocollimator on the entrance slit with an auxiliary lens.) The drum then was rotated to the other extreme (2400.0) and the autocollimator set up to line up with the Littrow mirror. After this the screw was returned again to the zero position and the mirror mount rotated on its seat to realign the mirror with the autocollimator. The fine adjustment in this operation was done with the screw, and the drum reading for which the mirror was in alignment was noted. At this drum

TABLE II(b). Indices of KDP in air, extraordinary ray.

Wavelength (Å)	Source	Observed index	Computed index	Residual $\times 10^4$
2138.560	Zn	1.54615	1.54612	0.2
2536.519	Low-pressure Hg	1.51586	1.51594	−0.7
2800.869	Zn	1.50416	1.50419	−0.2
2980.628	Cd	1.49824	1.49826	−0.2
3021.499	Hg	1.49708	1.49708	0.0
3035.781	Zn	1.49667	1.49668	−0.1
3125.663	Zn	1.49434	1.49432	0.2
3131.545	Hg	1.49419	1.49418	0.1
3341.478	Hg	1.48954	1.48952	0.2
3650.146	Hg	1.48432	1.48425	0.7
3654.833	Hg	1.48423	1.48418	0.5
3662.878	Hg	1.48409	1.48406	0.3
3906.410	Hg	1.48089	1.48088	0.2
4046.561	Hg	1.47927	1.47932	−0.4
4077.811	Hg	1.47898	1.47899	−0.1
4358.350	Hg	1.47640	1.47640	0.0
4916.036	Hg	1.47254	1.47254	0.0
5460.740	Hg	1.46982	1.46985	−0.3
5790.654	Hg	1.46856	1.46857	−0.1
6328.160	Laser	1.46685	1.46686	−0.1
10 139.75	Hg	1.46041	1.46043	−0.2
11 287.04	Hg	1.45917	1.45918	−0.1
11 522.76	Laser	1.45893	1.45893	−0.0
15 231.00	Laser	1.45521	1.45519	0.2
15 295.25	Hg	1.45512	1.45512	−0.1

TABLE III(a). Indices of ADP in air, ordinary ray.

Wavelength (Å)	Source	Observed index	Computed index	Residual $\times 10^4$
2138.560	Zn	1.62598	1.62591	0.7
2288.018	Cd	1.60785	1.60794	−0.9
2536.519	Low-pressure Hg	1.58688	1.58691	−0.4
2967.278	Hg	1.56462	1.56471	−0.9
3021.499	Hg	1.56270	1.56269	0.1
3125.663	Zn	1.55917	1.55915	0.2
3131.545	Hg	1.55897	1.55896	0.1
3341.478	Hg	1.55300	1.55296	0.4
3650.146	Hg	1.54615	1.54613	0.3
3654.833	Hg	1.54608	1.54604	0.4
3662.878	Hg	1.54592	1.54588	0.4
3906.410	Hg	1.54174	1.54171	0.3
4046.561	Hg	1.53969	1.53965	0.5
4077.811	Hg	1.53925	1.53922	0.3
4358.350	Hg	1.53578	1.53575	0.3
5460.740	Hg	1.52662	1.52659	0.3
5769.590	Hg	1.52478	1.52477	0.1
5790.654	Hg	1.52466	1.52465	0.0
6328.160	Laser	1.52166	1.52193	−2.8
10 139.75	Hg	1.50835	1.50825	1.0
11 287.04	Hg	1.50446	1.50446	0.0
11 522.76	Laser	1.50364	1.50366	−0.3

TABLE III(b). Indices of ADP in air, extraordinary ray.

Wavelength (Å)	Source	Observed index	Computed index	Residual $\times 10^4$
2138.560	Zn	1.56738	1.56730	0.8
2288.018	Cd	1.55138	1.55148	−1.0
2536.519	Low-pressure Hg	1.53289	1.53295	−0.6
2967.278	Hg	1.51339	1.51340	−0.1
3021.499	Hg	1.51163	1.51163	0.0
3125.663	Zn	1.50853	1.50852	0.1
3131.545	Hg	1.50832	1.50835	−0.3
3341.478	Hg	1.50313	1.50310	0.3
3650.146	Hg	1.49720	1.49715	0.5
3654.833	Hg	1.49712	1.49708	0.4
3662.878	Hg	1.49698	1.49694	0.4
4046.561	Hg	1.49159	1.49157	0.2
4077.811	Hg	1.49123	1.49120	0.3
4358.350	Hg	1.48831	1.48826	0.5
4916.036	Hg	1.48390	1.48386	0.4
5460.740	Hg	1.48079	1.48076	0.3
5769.590	Hg	1.47939	1.47934	0.5
5790.654	Hg	1.47930	1.47925	0.5
6328.160	Laser	1.47685	1.47723	−3.8
10 139.75	Hg	1.46895	1.46889	0.6
11 287.04	Hg	1.46704	1.46704	0.0
11 522.76	Laser	1.46666	1.46666	0.0

TABLE IV(a). Values of the constants A, B, C, D, and E for indices with respect to air.

	KDP, e ray	KDP, o ray	ADP, e ray	ADP, o ray
A	2.132668	2.259276	2.163077	2.302484
B	8.637494×10^{-21}	1.009956×10^{-10}	9.670312×10^{-11}	1.117089×10^{-10}
C	8.142631×10^{9}	7.726408×10^{9}	7.785289×10^{9}	7.605372×10^{9}
D	8.069981×10^{4}	3.251305×10^{6}	1.451540×10^{6}	3.751806×10^{6}
E	2.500000×10^{3}	2.500000×10^{3}	2.500000×10^{3}	2.500000×10^{3}

see errata JOSA 55, p. 210, 1965

TABLE IV(b). Values for absolute indices.

A	2.133831	2.260476	2.164256	2.304124
B	8.653247×10^{-21}	1.011279×10^{-10}	9.687319×10^{-11}	1.114254×10^{-10}
C	8.134538×10^{9}	7.726552×10^{9}	7.777850×10^{9}	7.535483×10^{9}
D	8.069838×10^{4}	3.249268×10^{6}	1.451426×10^{6}	3.777142×10^{6}
E	2.500000×10^{3}	2.500000×10^{3}	2.500000×10^{3}	2.500000×10^{3}

reading, then, the angle between the mirror and the incident beam is equal to the angle corresponding to 2400 divisions on the drum. This procedure had to be repeated a number of times to obtain the desired angle.

A special table was made for the prism which allowed it to be rotated accurately. The position of the prism was adjusted to give approximately minimum deviation for a convenient wavelength (e.g. 5461 Å).

The angle of incidence was measured by lining up the face of the prism and the Littrow mirror with an autocollimator. Since the Littrow in some measurements could not be rotated far enough, an auxiliary mirror on the prism table was found helpful. For wavelengths below 3125 Å, the position of the prism was readjusted to give minimum deviation for approximately 2537 Å.

The detectors used were a 1P28 photomultiplier and a lead sulfide photoconductor.

The sources of radiant energy were: (1) A high-pressure mercury arc. (2) A low-pressure mercury arc. (3) A Philips uv zinc discharge lamp. (4) A Philips uv cadmium discharge lamp. (5) A Perkin-Elmer, Spectra-Physics model 111 gas laser operating at 6328 Å, 1.15 μ or 1.5 μ, alternate outputs.

The beam was chopped at 1440 cps and the signal from the detector was amplified and rectified using a phase-sensitive detector.

To determine the polarization of a given wavelength, normal "Polaroid" sheet was used in the visible, and types HNP'B (unsupported) and HR in the uv and ir, respectively.[10]

Two prisms were measured. One was made of ADP and was 43 mm high with triangle sides of 23 mm and an angle of 61° 41′ 47″. The other one was made of KDP and was 30 mm high with sides of 25 mm and an angle of 60° 14′ 04″. Both prisms were examined in a Twyman–Green interferometer and were found to be flat and homogeneous to better than a quarter of a wavelength except for some roll-off at the edge.

The direction of the optical axis was parallel to the top edge in both prisms to within a few minutes of arc.

[10] Obtained from the Polaroid Corporation, Cambridge, Massachusetts.

TABLE V(a). Absolute indices of KDP, ordinary ray.

Wavelength (Å)	Frequency (cm^{-1})	Observed, corrected to vacuum index	Computed index	Residual $\times10^4$
2139.234	46 745.70	1.60227	1.60222	0.5
2288.724	43 692.47	1.58595	1.58593	0.2
2447.646	40 855.58	1.57274	1.57285	−1.1
2464.813	40 571.03	1.57152	1.57163	−1.1
2537.281	39 412.27	1.56678	1.56684	−0.6
2801.694	35 692.69	1.55309	1.55312	−0.3
2981.498	33 540.19	1.54663	1.54620	4.3
3022.379	33 086.52	1.54478	1.54483	−0.4
3126.569	31 983.94	1.54162	1.54160	0.1
3132.453	31 923.86	1.54143	1.54143	−0.0
3651.186	27 388.36	1.52976	1.52976	0.0
3655.874	27 353.24	1.52967	1.52968	−0.1
3663.921	27 293.16	1.52952	1.52954	−0.2
4047.704	24 705.36	1.52384	1.52387	−0.3
4078.962	24 516.04	1.52344	1.52348	−0.4
4359.575	22 938.02	1.52033	1.52033	0.0
5462.258	18 307.45	1.51194	1.51202	−0.8
5771.190	17 327.45	1.51029	1.51038	−0.9
5792.260	17 264.42	1.51019	1.51027	−0.8
6329.910	15 798.01	1.50779	1.50782	−0.3
10 142.53	9859.473	1.49576	1.49563	1.3
11 290.13	8857.294	1.49246	1.49229	1.6
11 525.91	8676.105	1.49176	1.49160	1.7
13 574.41	7366.803	1.48496	1.48521	−2.5

TABLE V(b). Absolute indices of KDP, extraordinary ray.

Wavelength (Å)	Frequency (cm^{-1})	Observed, corrected to vacuum index	Computed index	Residual $\times10^4$
2139.234	46 745.70	1.54663	1.54661	0.2
2537.281	39 412.27	1.51632	1.51639	−0.7
2801.694	35 692.69	1.50460	1.50463	−0.2
2981.498	33 540.19	1.49868	1.49869	−0.2
3022.379	33 086.52	1.49752	1.49752	0.0
3036.665	32 930.86	1.49711	1.49712	−0.1
3126.569	31 983.94	1.49477	1.49476	0.2
3132.453	31 923.86	1.49462	1.49461	0.1
3342.439	29 918.27	1.48997	1.48995	0.2
3651.186	27 388.36	1.48475	1.48468	0.7
3655.874	27 353.24	1.48465	1.48461	0.5
3663.921	27 293.16	1.48451	1.48449	0.3
3907.517	25 591.70	1.48131	1.48130	0.2
4047.704	24 705.36	1.47969	1.47973	−0.4
4078.962	24 516.04	1.47940	1.47941	−0.1
4359.575	22 938.02	1.47682	1.47681	0.0
4917.408	20 335.92	1.47295	1.47295	0.0
5462.258	18 307.45	1.47023	1.47026	−0.3
5792.260	17 264.42	1.46896	1.46898	−0.1
6329.910	15 798.01	1.46725	1.46727	−0.1
10 142.53	9859.473	1.46081	1.46083	−0.2
11 290.13	8857.294	1.45957	1.45958	−0.1
11 525.91	8676.105	1.45933	1.45933	−0.0
15 235.16	6563.764	1.45561	1.45559	0.2
15 299.43	6536.191	1.45552	1.45552	−0.0

The measurements were made in a temperature-controlled room. The temperature during the measurements ranged from 24.6° to 24.9°C.

DATA REDUCTION AND RESULTS

The wavelength-drum readings obtained for each wavelength were plotted to find the position corresponding to the maximum. This position was then corrected

TABLE VI(a). Absolute indices of ADP, ordinary ray.

Wavelength (Å)	Frequency (cm^{-1})	Observed, corrected to vacuum index	Computed index	Residual $\times 10^4$
2139.234	46 745.70	1.62650	1.62644	0.5
2288.724	43 692.47	1.60835	1.60843	−0.8
2537.281	39 412.27	1.58735	1.58736	−0.1
2968.144	33 691.09	1.56508	1.56515	−0.8
3022.379	33 086.52	1.56315	1.56313	0.2
3126.569	31 983.94	1.55962	1.55959	0.3
3132.453	31 923.86	1.55942	1.55940	0.2
3342.439	29 918.27	1.55345	1.55341	0.4
3651.186	27 388.36	1.54660	1.54658	0.1
3655.874	27 353.24	1.54652	1.54649	0.2
3663.921	27 293.16	1.54636	1.54634	0.2
3907.517	25 591.70	1.54217	1.54217	0.1
4047.704	24 705.36	1.54013	1.54011	0.2
4078.962	24 516.04	1.53969	1.53968	0.1
4359.575	22 938.02	1.53621	1.53622	−0.1
5462.258	18 307.45	1.52704	1.52707	−0.2
5771.190	17 327.45	1.52520	1.52525	−0.4
5792.260	17 264.42	1.52508	1.52513	−0.5
10 142.53	9859.473	1.50876	1.50869	0.7
11 290.13	8857.294	1.50487	1.50488	−0.1
11 525.91	8676.105	1.50405	1.50408	−0.3

TABLE VI(b). Absolute indices of ADP, extraordinar ryay.

Wavelength (Å)	Frequency (cm^{-1})	Observed, corrected to vacuum index	Computed index	Residual $\times 10^4$
2139.234	46 745.70	1.56788	1.56780	0.8
2288.724	43 692.47	1.55186	1.55196	−1.0
2537.281	39 412.27	1.53335	1.53341	−0.6
2968.144	33 691.09	1.51384	1.51384	−0.1
3022.379	33 086.52	1.51207	1.51207	0.0
3126.569	31 983.94	1.50896	1.50895	0.1
3132.453	31 923.86	1.50876	1.50879	−0.3
3342.439	29 918.27	1.50357	1.50354	0.3
3651.186	27 388.36	1.49763	1.49758	0.5
3655.874	27 353.24	1.49754	1.49750	0.4
3663.921	27 293.16	1.49741	1.49737	0.4
4047.704	24 705.36	1.49202	1.49199	0.2
4078.962	24 516.04	1.49165	1.49162	0.3
4359.575	22 938.02	1.48872	1.48868	0.5
4917.408	20 335.92	1.48431	1.48427	0.4
5462.258	18 307.45	1.48120	1.48117	0.3
5771.190	17 327.45	1.47980	1.47975	0.5
5792.260	17 264.42	1.47972	1.47966	0.5
6329.910	15 798.01	1.47726	1.47764	−3.8
10 142.53	9859.473	1.46935	1.46929	0.6
11 290.13	8857.294	1.46744	1.46744	0.1
11 525.91	8676.105	1.46707	1.46706	0.0

using the calibration curve of the screw. Further data reduction was done by an iterative process in a computer. In this process, the computer assumes a value for the refractive index; using that with the other data (angle of the prism, incident angle, angle between the slits, drum reading, and screw calibration), it calculates the angle included by the incident beam and the returning beam at the Littrow mirror. Then using this calculated angle it calculates the refractive index. Since the angle at the Littrow mirror is a function of the refractive index, there is only one value of this angle for which the assumed and the calculated index are the same. That is the correct value of the index. In general, the assumed value will, of course, not be the correct one. The process is therefore repeated using the last computed value to start with. This is continued until the difference between the two index values used in one iteration is less than 5×10^{-7}. At this point the computed index is printed out. The wavelength corresponding to the particular index is also printed out. The wavelength values were taken from the *M.I.T. Wavelength Tables*[11] and the *American Institute of Physics Handbook*.[12] The wavelengths of the laser were obtained from the atomic energy levels published by the National Bureau of Standards.[13]

A curve of the general form

$$n^2=A+B\nu^2/(1-\nu^2/C)+D/(E-\nu^2),$$

where $\nu=1/\lambda$ in cm^{-1}, was then fitted to the index values using the method of differential correction in the computer.[14]

In the near-infrared the absorption in both ADP and KDP becomes appreciable and less and less of the volume of the prism is used. This may give rise to errors in the measurement, because the illumination of the aperture becomes unsymmetrical; eventually, of course, the measurement becomes impossible. To fit a good

TABLE VII. Refractive indices of ADP.

Wavelength (μ)	Index in air: Ordinary ray	Index in air: Extraordinary ray	Absolute index: Ordinary ray	Absolute index: Extraordinary ray
0.2000	1.648335	1.587012	1.649083	1.587632
0.3000	1.563478	1.512318	1.563951	1.512787
0.4000	1.540308	1.492136	1.540785	1.492571
0.5000	1.529792	1.483315	1.530276	1.483737
0.6000	1.523539	1.478412	1.524024	1.478828
0.7000	1.519047	1.475202	1.519528	1.475614
0.8000	1.515340	1.472818	1.515813	1.473227
0.9000	1.511969	1.470859	1.512433	1.471268
1.0000	1.508705	1.469123	1.509156	1.469530
1.1000	1.505418	1.467494	1.505853	1.467901
1.2000	1.502029	1.465904	1.502447	1.466311
1.3000	1.498490	1.464311	1.498888	1.464718
1.4000	1.494766	1.462687	1.495142	1.463094
1.5000	1.490834	1.461012	1.491187	1.461419
1.6000	1.486676	1.459272	1.487004	1.459679
1.7000	1.482279	1.457458	1.482580	1.457865
1.8000	1.477631	1.455562	1.477903	1.455970
1.9000	1.472724	1.453578	1.472965	1.453986
2.0000	1.467548	1.451501	1.467756	1.451910

[11] *M. I. T. Wavelength Tables* (John Wiley & Sons, Inc., New York, 1939).

[12] *American Institute of Physics Handbook* (McGraw-Hill Book Company, Inc., New York, 1957).

[13] Atomic Energy Levels, Natl. Bur. Std. (U.S.), Circ. 467, Vol. 1 (15 June 1949).

[14] Kaj. L. Nielson, *Methods in Numerical Analysis* (The Macmillan Company, New York, 1957), p. 309.

curve to the data, we would like to have values of the refractive index beyond the wavelengths which are absorbed too strongly to be measured by the prism method. For ADP this occurred at about 1.15 μ for both rays. For KDP it turned out to be 1.35 μ for the ordinary ray. The extraordinary ray could be measured out to 1.5 μ. Attenuated total reflectance data showed no definite infrared pole for either of the crystals. This agrees with the findings of Barker and Tinkham[15] who report that there are a number of absorptions, none of which are very strong. From the available data we assumed a pole at 20 μ. The curves, therefore, are four-constant fits, since E was assumed to be 25×10^4 in all cases.

As a check on the general procedure and the accuracy of the measurements, we measured the refractive index of fused silica (G.E. 101) for 10 wavelengths. The results of this measurement are shown in Table I, together with

TABLE VIII. Refractive indices of KDP.

Wavelength (μ)	Index in air: Ordinary ray	Index in air: Extraordinary ray	Absolute index: Ordinary ray	Absolute index: Extraordinary ray
0.2000	1.621996	1.563315	1.622630	1.563913
0.3000	1.545084	1.497691	1.545570	1.498153
0.4000	1.524035	1.479814	1.524481	1.480244
0.5000	1.514498	1.472068	1.514928	1.472486
0.6000	1.508851	1.467856	1.509274	1.468267
0.7000	1.504817	1.465193	1.505235	1.465601
0.8000	1.501508	1.463303	1.501924	1.463708
0.9000	1.498514	1.461830	1.498930	1.462234
1.0000	1.495628	1.460590	1.496044	1.460993
1.1000	1.492730	1.459481	1.493147	1.459884
1.2000	1.489751	1.458443	1.490169	1.458845
1.3000	1.486645	1.457436	1.487064	1.457838
1.4000	1.483381	1.456437	1.483803	1.456838
1.5000	1.479938	1.455427	1.480363	1.455829
1.6000	1.476302	1.454395	1.476729	1.454797
1.7000	1.472459	1.453333	1.472890	1.453735
1.8000	1.468400	1.452234	1.468834	1.452636
1.9000	1.464118	1.451093	1.464555	1.451495
2.0000	1.459603	1.449906	1.460044	1.450308

the indices for fused silica as computed by Rodney and Spindler.[16] The differences between the two values and the difference listed by Rodney and Spindler for an unspecified General Electric sample are also shown.

Table II gives the index values for KDP with respect to air. Table III lists the index values for ADP with respect to air. The values of the constants A, B, C, and D, for the different cases are listed in Table IV(a).

By multiplying the observed values at each wavelength with the index of refraction of air at that wavelength, the absolute indices of refraction of the crystals

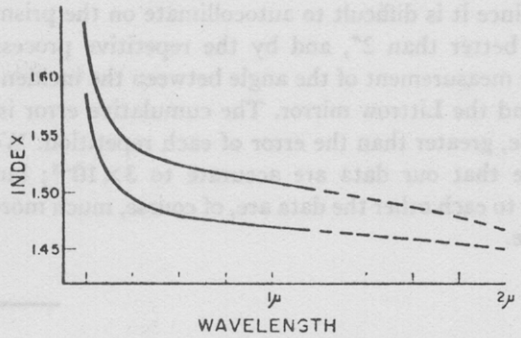

FIG. 1. Computed indices of ADP. Upper trace, ordinary ray. Curves are dashed in those spectral regions where no actual measurements were made.

were found. The indices of air were obtained from the table of wavenumbers published by the National Bureau of Standards.[17] The absolute values are listed as calculated values in Table V for KDP and in Table VI for ADP. Curves were fitted to these data, and from the constants of these curves the values listed in the third column of these tables were computed. The values of the constants A, B, C, and D are listed in Table IV(b).

Tables VII and VIII give values for the refractive indices of ADP and KDP at 19 wavelengths with equal wavelength increments between 2000 Å and 2 μ. These data are also shown graphically in Figs. 1 and 2.

ESTIMATED ERRORS

From the accuracies with which the different angles were measured, we can estimate the error in the final

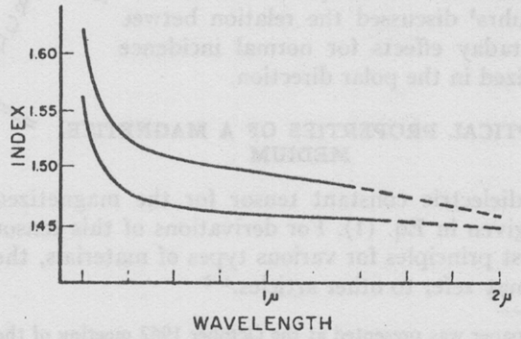

FIG. 2. Computed indices of KDP. Upper trace, ordinary ray. Curves are dashed in those spectral regions where no actual measurements were made.

value. The largest errors are undoubtedly caused by the relatively inaccurate measurement of the angle of inci-

[15] A. S. Barker and M. Tinkham, J. Chem. Phys. 38, 2257 (1963).

[16] W. S. Rodney, and R. J. Spindler, J. Opt. Soc. Am. 44, 677 (1954).

[17] "Table of Wavenumbers," Natl. Bur. Std. (U.S.) Monograph 3 (16 May 1960).

dence, since it is difficult to autocollimate on the prism face to better than 2″, and by the repetitive process used for measurement of the angle between the incident beam and the Littrow mirror. The cumulative error is, of course, greater than the error of each repetition. We estimate that our data are accurate to 3×10^{-5}; but relative to each other the data are, of course, much more accurate.

ACKNOWLEDGMENTS

The advice which Dr. N. I. Adams gave us in many stimulating discussions is gratefully acknowledged. We also would like to thank P. Kadakia who programmed the computer and P. B. Schoefer who found a number of errors.

Dr. R. W. Hannah kindly made the attenuated total reflectance measurements.

JOURNAL OF THE OPTICAL SOCIETY OF AMERICA NUMBER 10 OCTOBER 1964

Electromagnetic Theory of the Kerr ... cts for Oblique Incidence*

Department of Electrical En... ridge, Massachusetts

The Kerr ref... geneous is... tions to o... plied magn... single pass o... Faraday effect... transmission eff... ized slab of homo- dipole contribu- lab and the ap- ulations for a longitudinal first-order

INTRODU...

THIS paper considers the ... reflection relations for a ... medium in a uniform magnetic h... medium will be in the form of a slab ... lossless nonmagnetic media. Only o... portional to the first power of the magn... examined. Voigt[1,2] also has calculated t... tion coefficients for oblique incidence on ... face. Luhrs[3] discussed the relation betwee... and Faraday effects for normal incidence ... magnetized in the polar direction.

OPTICAL PROPERTIES OF A MAGNETIZE... MEDIUM

The dielectric constant tensor for the magnetized slab is given in Eq. (1). For derivations of this tensor from first principles for various types of materials, the reader may refer to other articles.[4–9]

$$\epsilon=\epsilon_0\begin{pmatrix}N^2+S & -iQ & 0\\ iQ & N^2+S & 0\\ 0 & 0 & N^2\end{pmatrix}. \quad (1)$$

...ized index of re- ...rtional to the magnetic ...ity Q is proportional to the ...esence of the anomalous Zeeman ...ponent of this tensor will contain a ...econd order in the magnetic field. This ...der contribution can be lumped into N^2, S, ... Q. That part that falls into N^2 and Q does not contribute to a first-order effect.

In the discussion of the equations that follow, the quantities N, Q, and S are assumed to be real and positive as for a diamagnetic glass. In general, these quantities can be complex and Q can be negative. The mathematical results are valid in these cases, although the interpretations would not apply.

The dielectric constant tensor is substituted into Maxwell's equations and a standard optical calculation is carried out as indicated in Eqs. (2), (3), (4), and (5) to find the index of refraction:

$$\nabla\times\mathbf{H}=i\omega\epsilon_0\kappa\mathbf{E}, \quad (2)$$

$$\nabla\times\mathbf{E}=-i\omega\mu_0\mathbf{H}. \quad (3)$$

Errata

54, 1215 (1964)

ZERNIKE, FRITS, JR. "Refractive Indices of Ammonium Dihydrogen Phosphate and Potassium Dihydrogen Phosphate between 2000 Å and 1.5 μ." The values of the observed indices of ADP at 6328 Å shown in Tables III(a), III(b), and VI(b) on pp. 1216–1217 are wrong. The value in Table III(a) should be 1.52193; that in Table III(b) should be 1.47727; that in Table VI(a) should be 1.52237 and that in Table VI(b) should be 1.47768. The constants given in Tables IV(a) and IV(b) should be changed correspondingly.

TABLE IV(a). Values of the constants A, B, C, D, and E with respect to air.

	ADP, e ray	ADP, o ray
A	2.163510	2.302842
B	9.616676×10^{-11}	1.1125165×10^{-10}
C	7.698751×10^{9}	7.5450861×10^{9}
D	1.479974×10^{6}	3.7753616×10^{6}
E	2.500000×10^{5}	2.500000×10^{5}

---

* This paper was presented at the October 1962 meeting of the Optical Society of America in Rochester, New York.

† Present address: American Optical Company, Research Division, Southbridge, Massachusetts 01550.

[1] W. Voigt, *Magneto- und Electro-Optik* (Teubner, Leipzig, 1908).

[2] W. Voigt, *Handbuch der Elektrizität und des Magnetismus*, edited by L. Graetz (Johann Ambrosius Barth, Leipzig, 1920), Vol. IV.

[3] C. H. Luhrs, Proc. IRE 40, 76 (1952).

[4] M. Born and P. Jordan, *Elementare Quantenmechanik* (Springer-Verlag, Berlin 1930).

[5] L. Rosenfeld, Z. Physik 57, 835 (1929).

[6] Y. R. Shen, Phys. Rev. 133, A511 (1964).

[7] R. Serber, Phys. Rev. 41, 489 (1932).

[8] J. Halpern, B. Lax, and Y. Nishina, Phys. Rev. 134, A140 (1964).

[9] P. N. Argyres, Phys. Rev. 97, 334 (1955).

Returning to the differential path difference introduced when the imperfectly adjusted shear plates are rotated, this is directly proportional to the angle through which the shear plates are turned. This effect is made use of in the type of path-difference compensator frequently used in the Rayleigh and Jamin refractometers. Because the shear produced by the shear plates also varies linearly with their rotation over the range used, the path difference introduced is proportional to the shear s. Thus if the phase of the transfer function of an optical system with coma is measured with the polarizing interferometer by noting the angle of the analyzer for maximum signal for various values of x, this is of the form:

$$\theta(s) \text{ measured} = (a+a')s+bs^3+\cdots,$$

where the a' takes account of the differential path difference introduced when the shear plates are rotated. If now $\theta(s)$ is plotted against s, then a measure of the phase distortion is obtained by the deviation of this curve from the straight line which is the tangent to the curve at $s=0$.

It is not possible to distinguish between a and a' in the above expression; this reflects the arbitrariness of phase measurements. There is no such thing as an absolute phase measurement, because there is no phase zero; if the arbitrarily chosen phase zero is changed, the factor "a" in the above expression is also changed. In terms of spread functions the lateral shifts of the spatial-frequency components are measured relative to the gaussian image point, but that this happens to be a convenient origin is the only reason for the choice.

It therefore appears that it would not be difficult to measure the argument of the transfer function for an optical system in the presence of coma with an interferometer. The tolerance of $\lambda/100$ previously applied to the differential path difference introduced by the rotation of the shear plates is unnecessary, although it is desirable for the differential path difference to be kept as small as possible, say $\lambda/10$, so that the phase distortion is at least comparable with the phase shift that is proportional to s.

ACKNOWLEDGMENT

I wish to express my gratitude to Dr. H. H. Hopkins for the many helpful discussions relating to this work and for his stimulating guidance during the three years he acted as my advisor.

JOURNAL OF THE OPTICAL SOCIETY OF AMERICA VOLUME 56, NUMBER 5 MAY 1966

Temperature Variation of the Index of Refraction of ADP, KDP, and Deuterated KDP*

RICHARD A. PHILLIPS

The Harrison M. Randall Laboratory of Physics, University of Michigan, Ann Arbor, Michigan 48107

(Received 21 September 1965)

The indices of refraction of ADP, KDP, and deuterated KDP were measured at temperatures between the Curie point and room temperature. The estimated accuracy of the data is ± 0.0001. The empirical equation $\Delta n = (n^2+an+b)c(298-T)$ where n is the index at room temperature, Δn is the change in index, and T is the temperature in °K, fits the measurements to within experimental error. The values of the constants a, b, and c are tabulated for each material, permitting n to be calculated for any temperature.

INDEX HEADINGS: Index of refraction; Nonlinear optics; Filters; Transmission; Birefringence.

I. INTRODUCTION

THE widespread use of ammonium dihydrogen phosphate (ADP), potassium dihydrogen phosphate (KDP), and deuterated KDP in nonlinear optical experiments[1] has prompted interest in precise measurements of their indices of refraction. Recently Zernike[2] reported measurements of the index of refraction of ADP and KDP at 24.8°C, accurate to 3×10^{-5} over the range 2138 Å to 1.529 μ. However, it is known[3] that at least one of the indices of refraction of ADP varies more than 2×10^{-5} for a 1C° change in temperature. During the course of some nonlinear optical experiments which the author is currently conducting, a need developed for measurements of the temperature dependence with an accuracy of 10^{-4}. These measurements were accomplished and the results are reported in this paper.

Evans[3] reported the shift in transmission wavelength with temperature of a Lyot filter constructed from ADP for 6562 Å at room temperature. From this information

* Work supported in part by the U. S. Atomic Energy Commission.

[1] For a general review of nonlinear optical phenomena see N. Bloembergen, *Nonlinear Optics* (W. A. Benjamin Inc., New York, 1965), or P. A. Franken and J. F. Ward, Rev. Mod. Phys. 35, 23 (1963).

[2] Frits Zernike. J. Opt. Soc. Am. 54, 1215 (1964), and corrections in J. Opt. Soc. Am. 55, 210E (1965).

[3] J. W. Evans, in *The Sun*, edited by G. P. Kuiper (University of Chicago Press, Chicago, 1953), p. 633.

the change per C° in the difference between the indices of refraction at the same wavelength, i.e., the change per C° in the birefringence, can be calculated as follows: The condition for transmission through a Lyot filter is

$$m\lambda = l(n_o - n_e), \quad (1)$$

where λ is the wavelength, m the order number, l the length of birefringent material out of which the filter is constructed, n_o the ordinary index of refraction, and n_e the extraordinary index of refraction. The change in transmitted wavelength produced by a change in temperature is then given by

$$d\lambda/dT = (l/m)\{\partial(n_o - n_e)/\partial T + (n_o - n_e)(1/l)(\partial l/\partial T)\}. \quad (2)$$

With the substitution

$$l/m = \lambda/(n_o - n_e), \quad (3)$$

Eq. (2) can be rewritten

$$\partial(n_o - n_e)/\partial T = [(n_o - n_e)/\lambda](d\lambda/dT) - (n_o - n_e)(1/l)(\partial l/\partial T). \quad (4)$$

Evans[3] reports $d\lambda/dT = 7.0$(Å/C°) for $\lambda = 6562$ Å and the index of refraction data[2] yield $n_o - n_e = 0.0447$. The second term on the right-hand side of Eq. (4) is negligible compared with the first for characteristic values of $(1/l)(\partial l/\partial T)$. Thus a numerical evaluation can be developed for ADP at room temperature:

$$\partial(n_o - n_e)/\partial T = -4.8 \times 10^{-5} \text{ per C°}. \quad (5)$$

Zwicker and Scherrer[4] measured the change in birefringence as a function of temperature at 5461 Å for KDP and deuterated KDP. Their measurements were from room temperature to 80°K, and showed an approximately linear relationship except for the region near the Curie point. Their measurements are $(-1.20) \times 10^{-5}$ per C° and $(-0.58) \times 10^{-5}$ per C° for KDP and deuterated KDP, respectively.

Optical second-harmonic generation from ADP, KDP, and deuterated KDP were measured as a function of temperature by van der Ziel and Bloembergen.[5] From their data, they calculated the change in coherence length and subsequently the change in differences between the indices of refraction at the two wavelengths

TABLE I. Dimensions of the prisms used in this study.

Material	Height mm	Sides mm	Prism angle
ADP	41.3	22.2×31.8	43° 51′ 10″
KDP	27.5	22.8×22.8	59° 55′ 35″
deuterated KDP	13.5	13.5×13.5	59° 54′ 15″

[4] B. Zwicker and P. Scherrer, Helv. Phys. Acta 17, 346 (1944).
[5] J. P. van der Ziel and N. Bloembergen, Phys. Rev. 135, 1662 (1964).

TABLE II. Index of refraction measurements for ammonium dihydrogen phosphate, $NH_4H_2PO_4$. The indices are measured with respect to air. The estimated accuracy of all entries in this Table is ±0.0001.

Wavelength in Å	Index at 298°K n_o	Index at 298°K n_e	Increase at 201°K n_o	Increase at 201°K n_e	Increase at 150°K n_o	Increase at 150°K n_e
6907	1.5192	1.4753			0.0059	0.0002
6438	...	...	0.0039	0.0001	...	...
6234	1.5223	1.4775	...	...	0.0060	0.0003
5779[a]	1.5246	1.4792	0.0039	0.0001	0.0060	0.0003
5461	1.5265	1.4808	0.0040	0.0001	0.0062	0.0003
4916	1.5303	1.4838	0.0040	0.0001	0.0061	0.0003
4358	1.5357	1.4882	0.0041	0.0001	0.0063	0.0003
4078	1.5392	1.4912	...	...	...	...
4047	1.5396	1.4915	0.0043	0.0001	0.0067	0.0003
3653	1.5457	1.4970	...	...	...	...

[a] Weighted-mean of mercury doublet.

6934 Å and 3467 Å. Their results do not permit the direct calculation of the variation with temperature of either the birefringence or of any one index, but do serve as a useful check on some of the results of the present work.

II. EXPERIMENTAL APPARATUS

The indices of refraction of ADP, KDP, and deuterated KDP were determined at various temperatures with the method of minimum deviation. The prism angle A and the minimum angle of deviation δ_m for each spectral line were measured with a spectrometer and visual techniques. The index of refraction was then calculated from the equation

$$n = \sin[\delta_m + (A/2)]/\sin(A/2). \quad (6)$$

The dimensions of the three prisms used in the present work are shown in Table I.

The spectrometer was a table-top prism model manufactured by Franz, Schmidt, and Haensch of Berlin.

The spectral lines used for the measurements were obtained from a General Electric type H-4 mercury lamp and with an Osram cadmium lamp, both operated according to manufacturers' specifications.

The surfaces of the deuterated prism were polished using a sequence of 15, 6, 3, 1, and $\frac{1}{4}\,\mu$ diamond paste available from Buehler Ltd. Ordinary white bond writing paper was placed over an optical flat and used as the polishing surface, and in the early stages of polishing, alcohol was used as a lubricant. In the late stages of polishing, lubrication was provided by the carrier of the diamond paste. The center regions of the surfaces could be polished flat to within 5 wavelengths. Since the polishing was done by hand there was considerable roll-off at the edges of the surfaces. The best regions of the surfaces were selected by visual examination of reflected and transmitted images of a slit and the remainder of the surface was then blocked off. The deuterated sample was supplied by the Clevite Corporation; they estimate that the degree of deuteration is 90%.

TABLE III. Index of refraction measurements for potassium dihydrogen phosphate, KH_2PO_4. The indices are measured with respect to air. The estimated accuracy of all entries in this Table is ±0.0001.

Wavelength in Å	Index at 298°K		Increase at 201°K		Increase at 154°K	
	n_o	n_e	n_o	n_e	n_o	n_e
6907	1.5052	1.4655	0.0033	0.0022	0.0047	0.0034
6234	1.5079	1.4672	0.0033	0.0022	0.0048	0.0033
5791	1.5099	1.4686	0.0034	0.0023	0.0048	0.0033
5461	1.5117	1.4700	0.0034	0.0023	0.0049	0.0033
4916	1.5152	1.4727	0.0034	0.0023	0.0049	0.0033
4358	1.5200	1.4766	0.0034	0.0023	0.0048	0.0034
4078	1.5232	1.4792	0.0034	0.0023	0.0050	0.0034
4047	1.5235	1.4795	0.0035	0.0023	0.0051	0.0033
3653	1.5292	1.4843	0.0037	0.0024	...	...

TABLE V. Values of the constants a, b, c for determining the temperature change in index of refraction. The constants are defined by the equation $\Delta n = (n^2 + an + b)c(298 - T)$.

	a	b	c°K^{-1}
ADP			
ordinary	−3.0297	2.3004	0.713×10^{-2}
extraordinary	0	0	0.675×10^{-6}
KDP			
ordinary	0	−1.432	0.402×10^{-4}
extraordinary	0	−1.105	0.221×10^{-4}
deuterated KDP			
ordinary	0	−1.047	0.228×10^{-4}
extraordinary	0	0	0.955×10^{-5}

Measurements of the indices at room temperature were obtained by mounting the prisms directly on the turntable of the spectrometer. Then, measurements of the change of indices were obtained by placing the prisms inside a Dewar and mounting the whole assembly on the turntable. Room-temperature measurements inside the Dewar were subtracted from low-temperature measurements inside the Dewar in order to evaluate the temperature dependence of the indices of refraction. In this manner, errors introduced by wedging in the windows of the Dewar and by misalignment cancel out to first order. Second-order effects do not compromise the accuracy of the results.

Fixed temperatures were maintained in the dewar by using mixtures of solid–liquid chlorobenzene 228°K, solid CO_2–ethyl alcohol 201°K, and solid–liquid methyl bromide 154°K. A solid–liquid mixture of ethyl alcohol was used to obtain a temperature near the Curie point of ADP (148°K). The prisms were cooled for one hour before measurements were taken. Monitoring of the spectrum produced by the prism indicated that at the end of one hour equilibrium was well established.

III. RESULTS AND DATA REDUCTION

Measurements of the indices of refraction at room temperature and their increases at lower temperatures are presented in Table II for ADP, Table III for KDP, and Table IV for deuterated KDP. Of particular interest is the result that the extraordinary index n_e for ADP exhibits a very small temperature dependence in comparison with those of the other two crystals, even though the ordinary indices vary much the same in all three materials. This unusually small temperature dependence of the extraordinary index in ADP accounts for the correspondingly very large temperature effects in the birefringence of this crystal.

TABLE IV. Index of refraction measurements for potassium dideuterium phosphate, KD_2PO_4. The indices are measured with respect to air. The estimated accuracy of all entries in this Table is ±0.0001.

Wavelength in Å	Index at 298°K		Increase at 225°K	
	n_o	n_e	n_o	n_e
6907	1.5022	1.4639	0.0019	0.0014
6234	1.5044	1.4656	0.0020	0.0015
5779[a]	1.5063	1.4670	0.0019	0.0014
5461	1.5079	1.4683	0.0020	0.0015
4916	1.5111	1.4710	0.0020	0.0014
4358	1.5155	1.4747	0.0020	0.0015
4078	1.5185	1.4772	0.0020	0.0014
4047	1.5189	1.4776	0.0020	0.0014

[a] Weighted-mean of mercury doublet.

The data presented in this report indicate that refractive indices can be well represented by a linear function of temperature over the region under consideration; i.e., above the Curie point. This conclusion is consistent with the indications provided by other authors. For example, van der Ziel and Bloembergen[5] show that the differences in refractive indices have a linear temperature dependence. In Figs. 3 and 4 of Zwicker and Scherrer[4] the birefringence at 5461 Å is plotted against temperature, and the relationship is linear except near the Curie point. In the present work, we therefore attempted to fit the data with an empirical formula of the type

$$\Delta n = cf(n)\Delta T. \tag{7}$$

We found that the equation fits the data within the experimental error, using the functions

$$f(n) = n^2 + an + b, \tag{8}$$

and

$$\Delta T = (298°\text{K} - T). \tag{9}$$

The values of the constants a, b, and c are listed in Table V.

IV. DISCUSSION OF ERRORS

Errors may be estimated from the precision with which the angle can be measured and the reproducibility of those measurements. The divided circle of the spectrometer can be read with a vernier to 10″, which for a material of $n = 1.5$ and prism angle of 60° corresponds to a precision of $\pm3\times10^{-5}$ in the index of refraction. However the measurement of the angles of minimum deviation could be reproduced only to 30″ which corresponds to an error of 10^{-4} in the reported index data.

TABLE VI. Comparison of present work with other reported measurements of the change of indices of refraction with temperature.

Material	Quantity measured	Present work	Zwicker & Scherrer[4]	van der Ziel & Bloembergen[5]
KDP	$\frac{\Delta(n_{o\,5461}-n_{e\,5461})}{\Delta T}$	$1.1\pm0.1\times10^{-5}$	1.2×10^{-5}	
deuterated KDP	$\frac{\Delta(n_{o\,5461}-n_{e\,5461})}{\Delta T}$	$0.73\pm0.15\times10^{-5}$	0.58×10^{-5}	
ADP	$\frac{\Delta(n_{o\,6943}-n_{e\,2432})^{a}}{\Delta T}$	$4.0\pm0.1\times10^{-5}$		$4.3\pm0.3\times10^{-5}$

[a] The values for $n_{e\,2432}$ were obtained by extrapolation of the data in Table II.

The reproducibility of the angle measurements to 30″ is larger than the 10″ precision afforded by the instrument. The full precision of the instrument was not achieved principally because of the poor quality of the prism surfaces which broadened and distorted the image of the spectral lines making it difficult to locate their centers. It was quite difficult to obtain flat parallel surfaces, because these materials are quite soft and easily scratched. Pieces can readily chip out of the edges during polishing roll under the surface being polished and ruin the work of a whole afternoon.

An independent check on the present measurements of ADP and KDP at room temperature is provided by comparison with the data of Zernike[2] for which the stated accuracy is $\pm3\times10^{-5}$. The index determinations of the present report tend to be uniformly higher than the Zernike results by 10^{-4} throughout the measured region of 4000 to 7000 Å. One possible explanation of this discrepancy is that the temperature of the samples was different in the two sets of measurements by 3C°. Zernike made his measurements in a room in which the temperature varied less than 0.3C°. The temperature of the room in which the present measurements were made varied 5C° but it was monitored with an accuracy of 1.5C°, and the data were later corrected to 298°K. However, it is possible that the temperature of the sample may not have been equal to the temperature of the room in either this or in the other reported experiments. This could occur if thermal gradients existed across the room or if the sample absorbed heat from the source. Another source of error that might give a uniform shift to the results is the measurement of the prism angle. But a lack of precision in the measurement of prism angle is not likely to be large enough to account for the discrepancy. The prism angles were measured by autocollimation and were reproducible to 10″, which corresponds to a reproducibility in n of 3×10^{-5}.

An independent check of the accuracy of the measured change of index of refraction with temperature change is provided by the data of Zwicker and Scherrer[4] and van der Ziel and Bloembergen.[5] The comparison is shown in Table VI. The agreement with Zwicker and Scherrer's data on KDP is particularly satisfying. Van der Ziel and Bloembergen report a larger temperature effect for ADP than is reported in this paper. For example, when ADP was cooled from 298°K to 150°K they report what would correspond to a change in birefringence of 63×10^{-4} compared to the 60×10^{-4} measured in this report. However their estimated error[6] is $\pm4\times10^{-4}$ so the two measurements agree within experimental error.

We have concluded that the accuracies of the results of this report are principally limited by the quality of the surfaces of the prism and possible temperature variations of the prism during the course of measurements. We estimate that the reliability of the present measurements is $\pm10^{-4}$.

ACKNOWLEDGMENTS

It is a pleasure to thank Professor Peter A. Franken for his advice and suggestions. The loan of the ADP prism by Dr. S. Pellicore and the loan of the KDP and deuterated KDP prisms by Dr. R. H. Kingston are gratefully acknowledged.

[6] J. P. van der Ziel (private communication).

INDEX MATCHING POLAR ANGLE FOR KDP FROM EQUATIONS FOR INDEX OF ZERNIKE AND PHILLIPS

JDE

CLEVELAND CRYSTALS, INC.
MAIL: Box 3157, Euclid, Ohio 44117
PLANT: 19306 Redwood Ave., Cleveland, Ohio 44110
Tel: (216) 486 - 6100

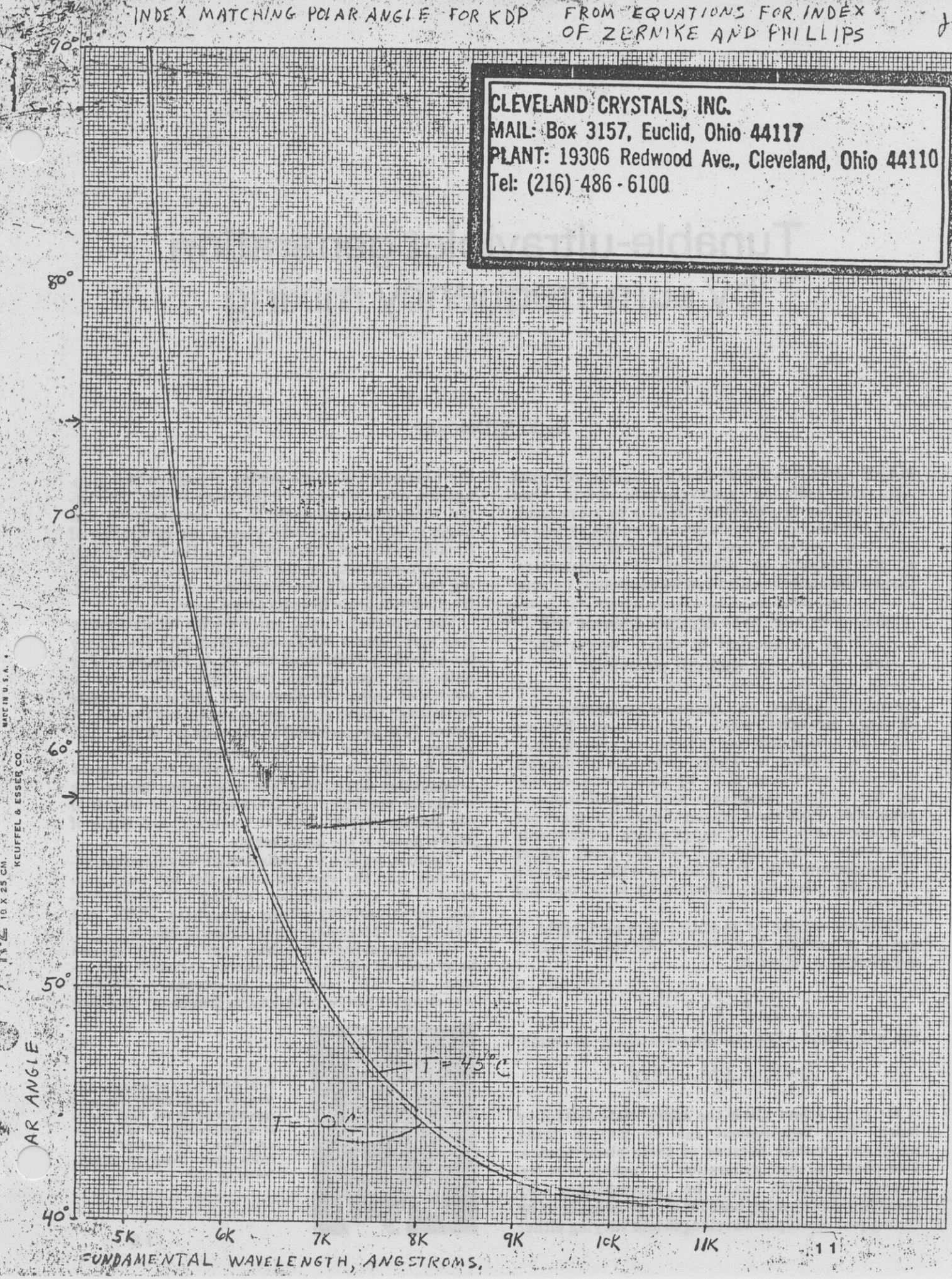

Tunable-ultraviolet generation by sum-frequency mixing

By F. B. Dunning

MANY APPLICATIONS require tunable, coherent ultraviolet radiation at wavelengths shorter than those that can be generated directly by a dye laser. Typically second-harmonic generation in a variety of nonlinear crystals is used to produce such radiation at wavelengths as short as 217 nanometers. Ultraviolet radiation also can be generated by sum-frequency mixing in nonlinear materials, but although straightforward, this technique has not found as wide application as harmonic generation.

Mixing in nonlinear crystals provide efficient uv generation at wavelengths extending into the vacuum ultraviolet

Recent studies in several laboratories suggest that ultraviolet generation by sum-frequency mixing has certain advantages over second-harmonic generation. Prominent among these advantages are a broader output-tuning range which extends into the vacuum ultraviolet and, in many cases, higher output powers. This article discusses the generation of tunable ultraviolet radiation by sum-frequency mixing.

Efficient mixing of radiation at wavelengths λ_1 and λ_2 to produce radiation at the sum-frequency wavelength λ_3 given by

$$\frac{1}{\lambda_3} = \frac{1}{\lambda_1} + \frac{1}{\lambda_2}$$

can only occur when the phasematching condition[1]

$$\frac{n(\lambda_3)}{\lambda_3} = \frac{n(\lambda_1)}{\lambda_1} + \frac{n(\lambda_2)}{\lambda_2}$$

is satisfied, where $n(\lambda)$ is the appropriate refractive index. This requirement can be met in many nonlinear crystals because of their birefringence. The phasematched generation of tunable sum-frequency radiation can be accomplished by simultaneously tuning both input wavelengths or by tuning just one input wavelength and varying either the temperature of the mixing crystal or the propagation direction of the interacting beams. The latter techniques, referred to as temperature and angle tuning respectively, permit the generation of tunable radiation either by mixing the fundamental and harmonic outputs of a single dye laser or by mixing the output of a dye laser with one of the fixed-frequency outputs from its pump laser.

The expected output powers with focused Gaussian input beams can be calculated with the theory developed by G.D. Boyd and D. A. Kleinman.[2] For unfocused input beams, the output power can be estimated using the plane-wave coupled-amplitude equations.[1] Under small-signal conditions the output power P_3 is proportional to the product of the input powers, P_1 and P_2. The conversion efficiency P_3/P_1P_2, depends on many parameters, including the propagation direction of the interacting beams, the nonlinear coefficient of the medium, the length of the mixing crystal, and the linewidth and angle of convergence of the input beams.

Tunable, pulsed uv radiation at wavelengths extending into the vacuum ultraviolet has been generated by sum-frequency mixing in ammonium- and potassium-dihydrogen phosphate (ADP and KDP)[3-7] and potassium pentaborate (KB5).[8-12]

Radiation at wavelengths longer than 246 nm can be generated efficiently by second-harmonic conversion in KDP and its isomorphs.[13] Shorter wavelengths can be produced by frequency doubling

F. B. Dunning *is an assistant professor at Rice University, with joint appointments in the departments of space physics and astronomy, and physics. He received a doctorate from University College London in 1969*

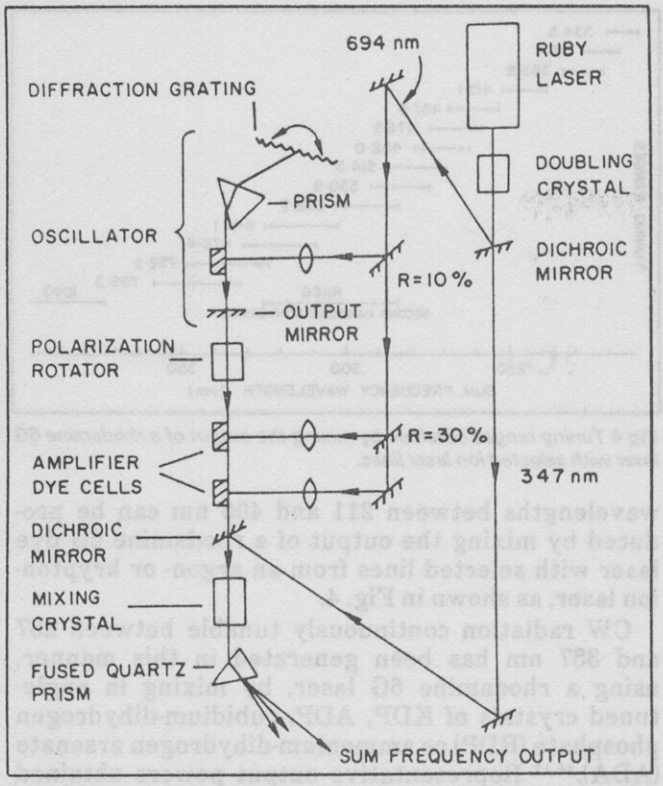

Fig 1 *Ruby-pumped dye-laser system generates radiation at 240 to 250 nm by sum-frequency mixing. The cover photograph shows this system being operated by Robert E. Stickel Jr.*

in lithium formate monohydrate (LFM) and KB5. Harmonic-conversion efficiencies in these materials are typically low, however, because of the strong uv absorption and low damage threshold of LFM,[14] and the small nonlinear coefficients of KB5.[15] The shortest wavelength that can be generated by frequency doubling in currently available materials is 217 nm.[15]

In certain cases, radiation at wavelengths that can be produced by frequency doubling can be more efficiently generated by mixing, resulting in higher output powers. This occurs when mixing permits better use of the pump-laser output, a more-efficient nonlinear medium, or a more-favorable phasematching angle.

Consider, for example, the generation of intense, tunable radiation in the range 240 to 250 nm with a ruby-pumped dye laser. The most efficient way to produce such radiation is not by frequency-doubling the output of a dye laser pumped by the ruby laser's second harmonic, but by mixing, in a temperature-tuned 90°-phasematched ADP crystal, the second harmonic of the ruby laser with the output of an infrared dye laser pumped by the ruby laser's fundamental output. The latter approach yields higher output power because it utilizes both the fundamental and harmonic outputs of the ruby laser, and because it allows use of an efficient nonlinear material and a favorable crystal orientation.

The laser system constructed in this laboratory[7] to generate tunable uv radiation in this manner for a series of photoionization experiments is shown in Fig. 1. Its complexity is comparable to that which would have been required had second-harmonic conversion been employed. Temperature-tuning curves for 90°-phasematched mixing with 347-nm radiation

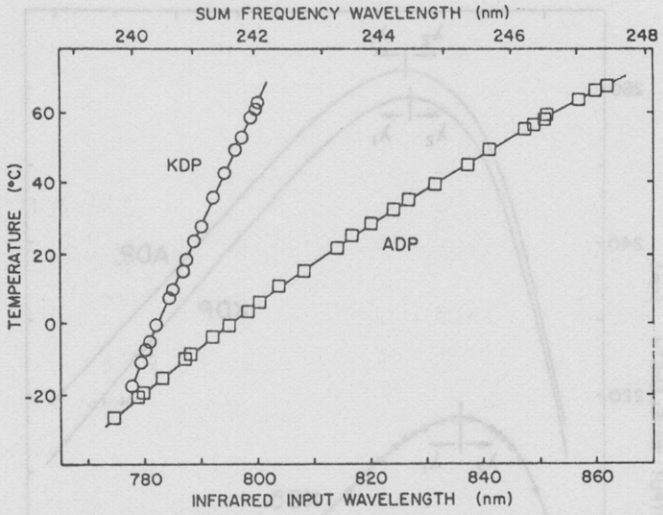

Fig 2 *Temperature-tuning curves for 90°-phasematched sum-frequency mixing of the output from an infrared dye laser (bottom scale) with 347-nm radiation in ADP and KDP*

in both KDP and ADP are shown in Fig. 2. As the figure indicates radiation can be generated across a considerable wavelength range with a temperature-tuned ADP crystal, and further refrigeration should extend the tuning range to about 236 nm as the Curie temperature of −125°C is approached. UV output energies of 30 millijoules, corresponding to pulse powers of about one megawatt, are obtained with the laser system shown in Fig. 1. Over-all efficiencies to 4% have been achieved for the conversion of ruby-laser radiation to the sum frequency.

Pushing to shorter wavelengths

Radiation at wavelengths too short to be produced by frequency doubling can be generated by mixing. The wavelength combinations λ_1 and λ_2 which produce phasematched sum-frequency mixing during propagation along the *b* axis of a KB5 crystal, together with those that produce 90°-phasematched mixing in room temperature ADP and KDP, are shown in Fig. 3. These directions of propagation yield the most efficient uv conversion, together with the shortest output wavelengths, that can be realized in each of the materials for a given input wavelength.

UV radiation tunable between 208 and 234 nm has been generated efficiently by mixing, in angle- and temperature-tuned crystals of ADP and KDP, the fundamental output of a neodymium-yag laser and the output of a frequency-doubled dye laser.[5] Because ADP is particularly sensitive to temperature tuning, as indicated in Fig. 2, the shortest putput wavelengths are obtained with a refrigerated ADP crystal. Wavelengths down to about 202 nm can be produced by mixing with 1,060-nm radiation in refrigerated ADP.[5]

Wavelengths as short as 185 nm, in the vacuum ultraviolet, have been produced by mixing in KB5.[12] Because KB5 is not strongly absorbing at this wavelength, or at the corresponding input wavelengths,[12] it should be possible to generate useful quantities of radiation at even shorter wavelengths in KB5. Although KB5 has a small nonlinear coefficient[15] its high damage threshold permits the use of large input-power densities, and

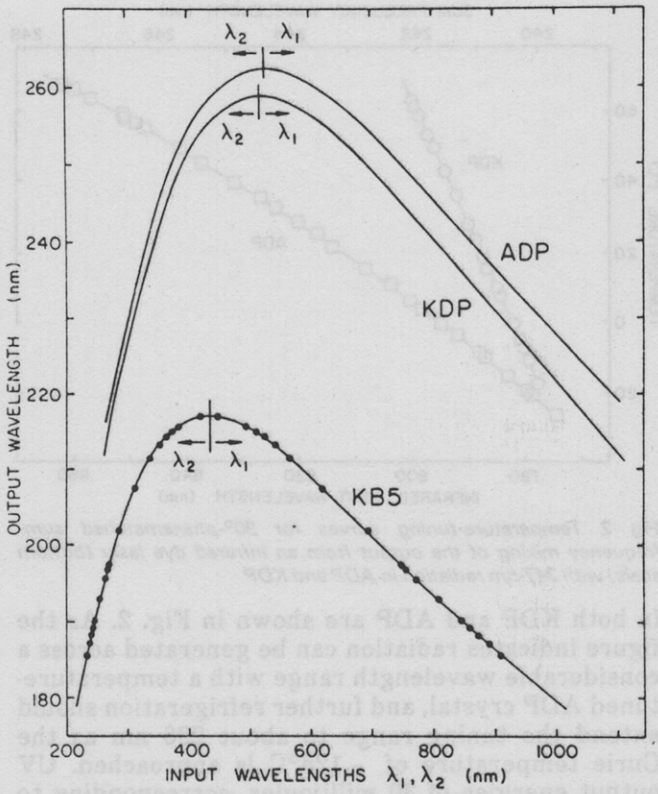

Fig 3 *Wavelength combinations λ_1 and λ_2 which produce phasematched sum-frequency mixing in ADP, KDP and KB5 for the phasematching conditions described in the text*

as a result sizable output powers can be obtained,[10,11] Efficiencies of about 10% for the upconversion of ultraviolet input radiation to sum-frequency radiation have been realized in KB5 when the interacting beams propagate along the *b* axis.[9,11]

Tunable ultraviolet radiation also has been generated by mixing in angle-tuned KB5 crystals. Radiation tunable between 197 and 199 nm has been produced, with peak powers to 40 kilowatts, by mixing the fourth harmonic of a Nd-yag laser with output of an infrared dye laser.[10] In other investigations radiation tunable between 201 and 212 nm has been produced by mixing the fundamental output of a ruby laser with uv radiation from a frequency-doubled dye laser,[9] and intense 207- to 217-nm radiation has been generated by mixing the fundamental and second-harmonic outputs of a high-power dye laser.[11] These studies show that angle tuning in the *ab* plane provides a considerable output tuning range, although the uv conversion efficiency decreases rapidly as the angle between the interacting beams and the *b* axis increases.

CW ultraviolet generation

Continuouswave radiation tunable across a wide wavelength range may be generated simply and conveniently by mixing the output of a commercial cw dye laser with various output lines from an argon- or krypton-ion laser in a nonlinear crystal located outside both laser cavities. Because ion lasers provide lines at wavelengths between the ultraviolet and the infrared, a wide range of sum-frequency wavelengths can be obtained without changing the dye or optics in the cw laser and without use of the less-efficient coumarin dyes. For example,

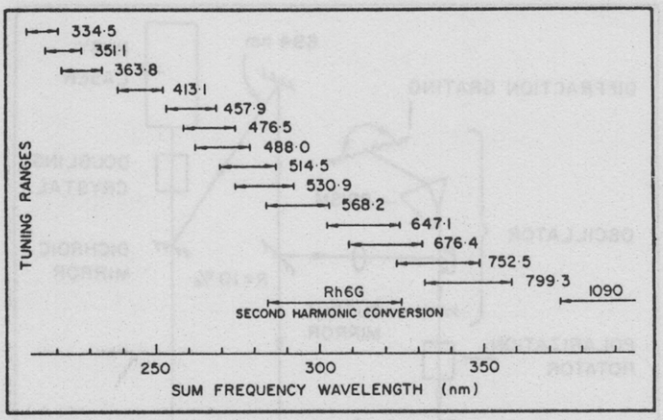

Fig 4 *Tuning ranges obtained by mixing the output of a rhodamine 6G laser with selected ion laser lines.*

wavelengths between 211 and 406 nm can be produced by mixing the output of a rhodamine 6G dye laser with selected lines from an argon- or krypton-ion laser, as shown in Fig. 4.

CW radiation continuously tunable between 257 and 357 nm has been generated in this manner, using a rhodamine 6G laser, by mixing in angle-tuned crystals of KDP, ADP, rubidium-dihydrogen phosphate (RDP) or ammonium-dihydrogen arsenate (ADA).[16,17] Representative output powers obtained both by frequency mixing, and by direct frequency doubling of the output of the rhodamine 6G laser, in these crystals are shown in Fig. 5 as a function of the output wavelength, together with the corresponding phasematching angles.

Because UV conversion efficiency is highest for phasematching angles θ close to 90° the best choice for a mixing medium depends on the output wavelength required. The efficencies realized under optimum focusing conditions[2] in the different crystals (each 25 millimeters long) were approximately equal at the same phasematching angle. Typical values, which range from about 10^{-3} per watt at θ = 90° to about 5×10^{-5} W^{-1} at θ = 60°, are included in Fig. 5. These efficiencies are sufficient for generation of output powers in excess of 0.1 milliwatt across a significant wavelength range given the input powers typically available from rhodamine 6G and ion lasers.

Continuouswave radiation at wavelengths shorter than 257 nm has been obtained by mixing in an angle-tuned KB5 crystal.[18] Radiation tunable between 211 and 215 nm has been produced by mixing the output of a rhodamine 6G laser with the 334.5-nm line of an argon-ion laser. Radiation extending to about 233 nm can be generated in KB5 by mixing with the other ultraviolet lines of an argon-ion laser. The uv conversion efficiencies obtained are low, less than 10^{-5} W^{-1}, because of the low nonlinear coefficient of KB5, but output powers in excess of 10 nanowatts have been realized.[18]

Higher output powers can be obtained in certain wavelength intervals with dyes other than rhodamine 6G. For example, mixing the output of a rhodamine 110 laser with the 351.1-nm argon line provides higher powers in the range 213 to 217 nm.[18] The choice of the best dye to use to generate a particular range of ultraviolet wavelengths depends on such considerations as the efficiency of the dye, the

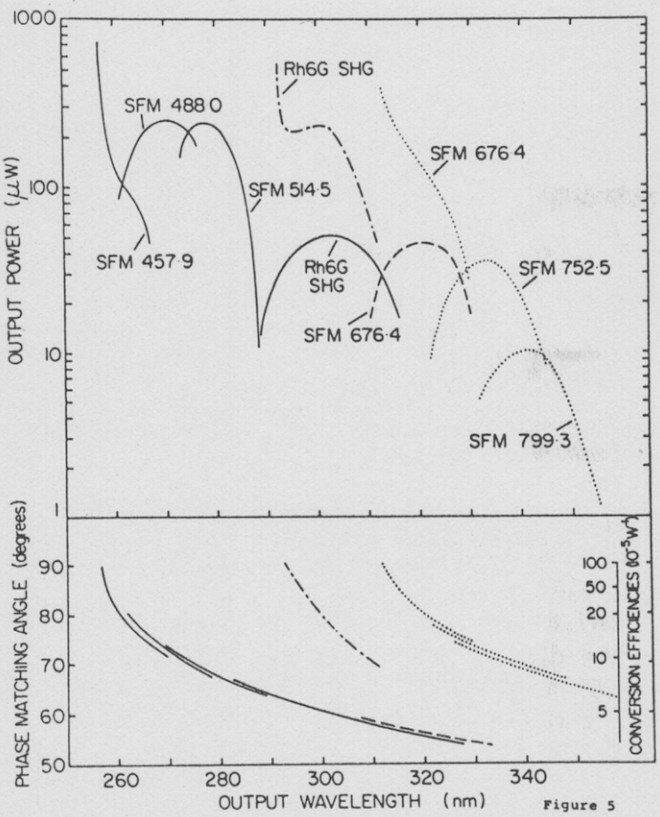

Fig 5 *Representative data for the generation of ultraviolet radiation by extracavity second-harmonic conversion and sum-frequency mixing using a rhodamine 6G laser. Solid line is KDP, dashed-and-dotted line ADA, dashed line ADP and dotted line RDP*

intensity of the ion-laser lines with which the dye-laser output must be mixed, and the uv conversion efficiency possible with a particular combination of input wavelengths. Many nonlinear materials are available besides those which have been employed in cw mixing studies to date, and their use should also be considered.

As is evident from the above discussion, sum-frequency mixing can provide both pulsed and cw coherent radiation across an extended range in the ultraviolet. Because of this, frequency-mixing techniques are worth consideration in any application requiring a source of tunable uv radiation.

References

1. F. Zernike and J. E. Midwinter, in *Applied Nonlinear Optics* A. A. Ballard ed (Wiley, New York, 1973)
2. G. D. Boyd and D. A. Kleinman *J Appl Phys 39* 3597 (1968)
3. R. W. Wallace *Opt Comm 4* 316 (1971); E. S. Yeung and C. B. Moore *J Am Chem Soc 93* 2059 (1971)
4. G. A. Massey *Appl Phys Lett 24* 371 (1974)
5. G. A. Massey and J. C. Johnson *IEEE J Quantum Electron QE12* 721 (1976)
6. I. M. Beterov et al *Opt Comm 19* 329 (1976)
7. R. E. Stickel Jr. and F. B. Dunning *Appl Opt* (Apr 15, 1978)
8. F. B. Dunning and R. E. Stickel Jr. *Appl Opt 15* 3131 (1976)
9. R. E. Stickel Jr. and F. B. Dunning *Appl Opt 16* 2356 (1977)
10. K. Kato *Appl Phys Lett 30* 583 (1977)
11. K. Kato *IEEE J Quantum Electron QE13* 544 (1977)
12. R. E. Stickel Jr. and F. B. Dunning *Appl Opt* (Apr 1, 1978)
13. R. K. Jain and T. K. Gustafson *IEEE J Quantum Electron QE12* 555 (1976)
14. F. B. Dunning, F. K. Tittel and R. F. Stebbings *Opt Comm 7* 181 (1973)
15. H. J. Dewey *IEEE J Qunatum Electron QE12* 303 (1976)
16. S. Blit et al *Opt Lett 1* 58 (1977)
17. S. Blit et al, *Appl Opt 17* 721 (1978)
18. R. E. Stickel Jr. et al, to be submitted for publication.

Appl 17 981 (78)
Opt

Reprinted from Laser Focus Magazine
May 1978, pages 72-76
Advanced Technology Publications
1001 Watertown Street, Newton, MA 02165
(617) 244-2939